

Article

Machine Learning and Transformers for Thyroid Carcinoma Diagnosis

Yassine Habchi , Hamza Kheddar , Yassine Himeur , Mohamed Chahine Ghanem 

¹ Institute of Technology, University Center Salhi Ahmed, Naama, Algeria.

² LSEA Laboratory, Electrical Engineering Department, University of Medea, 26000, Algeria.

³ College of Engineering and Information Technology, University of Dubai, Dubai, UAE.

⁴ Cybersecurity Institute, Department of Computer Science, University of Liverpool, Liverpool, UK.

* Correspondence: mohamed.chahine.ghanem@liverpool.ac.uk

Abstract: The growing interest in developing smart diagnostic systems to help medical experts process extensive data for treating incurable diseases has been notable. In particular, the challenge of identifying thyroid cancer (TC) has seen progress with the use of machine learning (ML) and big data analysis, incorporating Transformers to evaluate TC prognosis and determine the risk of malignancy in individuals. This review article presents a summary of various studies on AI-based approaches, especially those employing Transformers, for diagnosing TC. It introduces a new categorization system for these methods based on artificial intelligence (AI) algorithms, the goals of the framework, and the computing environments used. Additionally, it scrutinizes and contrasts the available TC datasets by their features. The paper highlights the importance of AI instruments in aiding the diagnosis and treatment of TC through supervised, unsupervised, or mixed approaches, with a special focus on the ongoing importance of Transformers and large language models (LLMs) in medical diagnostics and disease management. It further discusses the progress made and the continuing obstacles in this area. Lastly, it explores future directions and focuses within this research field.

Keywords: Thyroid carcinoma detection; Artificial intelligence; Deep learning; Biomedical images; Transformers; Large language model.

1. Introduction

The integration of artificial intelligence (AI) into the healthcare sector represents a pivotal advancement, fundamentally altering the landscape of medical diagnostics, therapy, and patient management. The superior capabilities of AI, incorporating the identification of patterns, forecasting analytics, and the process of making decisions, have led to the creation of systems that can interpret intricate medical data with greater accuracy and scale than ever before [1,2]. Such advancements facilitate the early identification of diseases, enhance the accuracy of diagnoses, and support the customization of treatment plans for individuals. In addition, predictive models powered by AI are capable of foreseeing disease spread, boosting the efficiency of healthcare operations, and significantly improving outcomes for patients [3]. AI also has the potential to make healthcare more equitable by reducing disparities in service quality between rural and urban areas, thus improving access to premium healthcare services. As a result, the role of AI is significant in healthcare and is anticipated to grow as ongoing technological innovations lead to the creation of even more advanced applications, promising widespread benefits for patient health across the globe [4,5].

Nonetheless, the trust serves as a critical intermediary, impacting the extent to which factors related to AI affect user acceptance. Research has explored the roles of trust, risk, and security in determining the uptake of AI-powered support [6]. Empirical investigations within these studies have underscored the essential influence of trust in forming the basis

Citation: Habchi, et al. Machine Learning and Transformers for Thyroid Carcinoma Diagnosis. *Mach. Learn. Knowl. Extr.* **2025**, *1*, 0. <https://doi.org/>

Firstname Lastname

Received: 13 April 2025

Accepted:

Published:

Copyright: © 2025 by the authors. Submitted to *Mach. Learn. Knowl. Extr.* for possible open access publication under the terms and conditions of the Creative Commons Attribution (CC BY) license (<https://creativecommons.org/licenses/by/4.0/>).

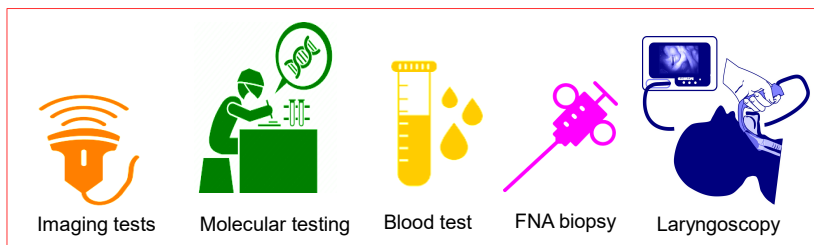


Figure 1. Approaches for identifying TC.

of user acceptance. Cancer is marked by the unchecked growth of cells across various parts of the body. These cells multiply erratically and can spread, damaging healthy tissue [7]. Such uncontrolled cell growth is triggered by changes or mutations in the DNA of these cells [8]. The DNA in cells comprises multiple genes, which provide the instructions necessary for a cell's function, growth, and division. When these instructions are erroneous, it can interrupt the normal functioning of cells and may result in the development of cancer [9]. Thyroid cancer (TC), in particular, is recognized as one of the most common types of endocrine malignancies around the globe [10].

Recent global epidemiological studies indicate a rise in abnormal thyroid nodule (TN), linked to an upsurge in genetic cellular activity. This suggests an increase in normal cell functions, with anomalies classified into four primary types: follicular thyroid carcinoma (FTC), papillary carcinoma (PTC), medullary thyroid carcinoma (MTC), and anaplastic thyroid carcinoma (ATC) [11–14]. Elements like exposure to radiation, Hashimoto's thyroiditis, psychological factors, and genetic components, alongside advances in technologies of detection, appear in these cancers. These factors can cause chronic health issues like diabetes and blood pressure instability. The cell cancer volume is key to evaluating the aggressiveness and prognosis of TC's, with cell nuclei detection offering alternative markers for evaluating cancer cell proliferation. Computer-aided diagnosis (CAD) systems have gained prominence in thyroid cancer diagnosis (TCD) analysis, improving diagnostic accuracy and reducing interpretation times [15]. Radiomics, particularly through ultrasound (US) imaging [16], has emerged as an efficient diagnostic method. The American College of Radiology's thyroid imaging reporting and data system (TIRADS) categorizes TNs from benign to malignant [17]. Despite available open-source tools for nodule analysis, accurately identifying them remains a challenge, reliant on radiologists' experience and the subjective nature of visual image analysis [18].

Additionally, US imaging can be a lengthy and stress-inducing process, which may result in incorrect diagnoses. It is common to encounter classification errors among cases deemed normal, benign, malignant, or of uncertain nature [19,20]. For a more precise diagnosis, a fine-needle aspiration biopsy (FNAB) is often conducted. Yet, this technique can be uncomfortable for patients, and inaccuracies by the practitioner can mistakenly label benign nodules as malignant, leading to unnecessary costs [21]. The main issue is the selection of nodule characteristics critical for accurately differentiating between benign and malignant cancer. Various research efforts have delved into the use of conventional US imaging to characterize different types of cancers, such as retinal [22], breast [23], and thyroid [24]. Despite these efforts, there remains a lack of accuracy in the methods available for effectively categorizing TNs, as depicted in Figure 1.

The deployment of AI technology is crucial in diminishing subjectivity and boosting the precision of pathological assessments, particularly for complex conditions like thyroid diseases [25]. These advancements enhance the analysis of images obtained through US and expedite analysis times. Machine learning (ML) and deep learning (DL) stand out as effective AI-based strategies for automating the differentiation of TNs in various contexts, including US, fine-needle aspiration, and during thyroid surgical procedures [26].

Traditional methods for diagnosing TC, like fine-needle aspiration biopsies, can often produce ambiguous outcomes, whereas AI presents an opportunity for more accurate

and less invasive alternatives. This review seeks to integrate insights from pathology, computer science, oncology, and radiology, encouraging cross-disciplinary collaboration. It will also explore the clinical significance of AI, offering recommendations for healthcare professionals on utilizing AI advancements for improving patient care, and pinpointing directions for future research endeavours. Additionally, the review discusses the healthcare and economic system benefits, including cost savings and reduced wait times. Yet, it's essential to confront the challenges AI brings, such as ethical considerations and data privacy, to facilitate its responsible integration into healthcare practices. This review aims to provide an extensive examination of AI's current and future impact on the detection of TC, serving as a resource for both researchers and clinicians.

1.1. Contribution of the paper

This review explores the use of AI in identifying TC, emphasizing the shift towards improved diagnostic accuracy using AI techniques in healthcare, specifically for detecting TC. It begins with an overview of current frameworks and delves into AI strategies such as supervised learning (SL), unsupervised learning (USL) like clustering, and ensemble methods (EMs) like boosting and bagging, ML, DL, vision Transformer s (ViTs), large language models (LLMs). The significance of comprehensive datasets for AI success is discussed, alongside an analysis of TCD, feature selection, and extraction methods. It evaluates AI effectiveness in TCD through various metrics and concludes by highlighting future research directions to overcome challenges and enhance AI deployment in TCD. The review underscores AI's potential to revolutionize TCD, advocating for ongoing assessment to ensure ethical and effective use.

The main advancements presented in our paper are:

- A review of current frameworks coupled with a detailed investigation into diverse AI strategies, including SL, conventional classification, USL, DL, Transformers, and LLMs techniques.
- An in-depth review of various TCDs, detailing their attributes and examining methods for feature selection and extraction used in different studies.
- A detailed discussion on the benchmark criteria for assessing the efficacy of AI-powered approaches in identifying TC. These evaluation metrics cover a wide range, from regression and classification parameters to statistical, computer vision, and ranking parameters.
- A thorough critique and exploration of the challenges, limitations, prevalent trends, and unresolved questions in the domain.
- An analysis of future research priorities, highlighting specific areas that require further investigation to address current challenges and improve methods for detecting TC.
- A spotlight on the transformative impact of AI in enhancing TC diagnosis, stressing the importance of continual critical review to ensure its ethical and effective application.

Additionally, the main contributions of this review, as differentiated from other reviews, are summarized in Table 1.

1.2. Bibliometric analysis

A bibliometric analysis was performed to delve into and evaluate the scientific studies reviewed in this paper. The continuous interest in AI-based TC research is depicted in Figure 2, with the publication count reaching 81 in 2022. Figure 2 (a) highlights the leading researchers in the field of TC-oriented AI research, focusing on those who have published within the past five years. Figure 2 (b) provides a snapshot of the enduring interest in AI-based TCD research, showcasing a rising trend in the creation of AI solutions for TC prognosis and diagnosis since 2015. Figure 2 (c) maps out the countries that are major contributors to the research output in this area, with China and the United States showing a pronounced focus on AI-driven TC detection. Lastly, Figure 2 (d) illustrates the breakdown

Table 1. The notable advancements made by the suggested review in the categorization of TC when contrasted with similar research endeavours.

Ref	Year	Patient privacy	TC detect. schemes	AI apps	ML	DL	Trans	LLM	F	TCE	Prospective path					Metric
											IoMIT	RS	RL	PS	XAI	
[27]	2021	✓	✓	✗	✗	✗	✓	✗	✓	✗	✗	✗	✗	✗	✗	✗
[28]	2021	✓	✓	✗	✗	✗	✓	✗	✗	✗	✗	✗	✗	✗	✗	✗
[29]	2021	✓	✓	✗	✗	✓	✓	✗	✓	✓	✗	✗	✗	✗	✓	✓
[30]	2021	✓	✓	✗	✗	✗	✓	✗	✗	✗	✗	✗	✗	✗	✓	✓
[31]	2021	✓	✓	✗	✗	✓	✓	✗	✗	✗	✗	✗	✗	✗	✓	✓
[32]	2022	✓	✓	✗	✗	✗	✓	✗	✗	✗	✗	✗	✗	✗	✗	✓
[33]	2022	✓	✓	✗	✗	✗	✓	✗	✗	✗	✗	✗	✗	✗	✓	✗
[34]	2022	✓	✓	✗	✗	✓	✓	✗	✓	✗	✗	✗	✗	✗	✓	✓
[35]	2022	✓	✓	✗	✗	✓	✓	✗	✓	✗	✗	✗	✗	✗	✓	✓
Our	2024	✓	✓	✗	✗	✓	✓	✗	✓	✓	✓	✓	✓	✓	✓	✓

Abbreviations: Artificial intelligence applications (AI apps); Transformers (Trans.); Features (F); TC example (TCE); Internet of medical imaging thing (IoMT); Recommender systems (RS); Reinforcement learning (RL); Panoptic segmentation (PS); Edge, fog and cloud networks based on AI (EFC-AI).

of publication types, with journal articles making up the bulk of the research (67.2%), followed by conference papers (19.3%).

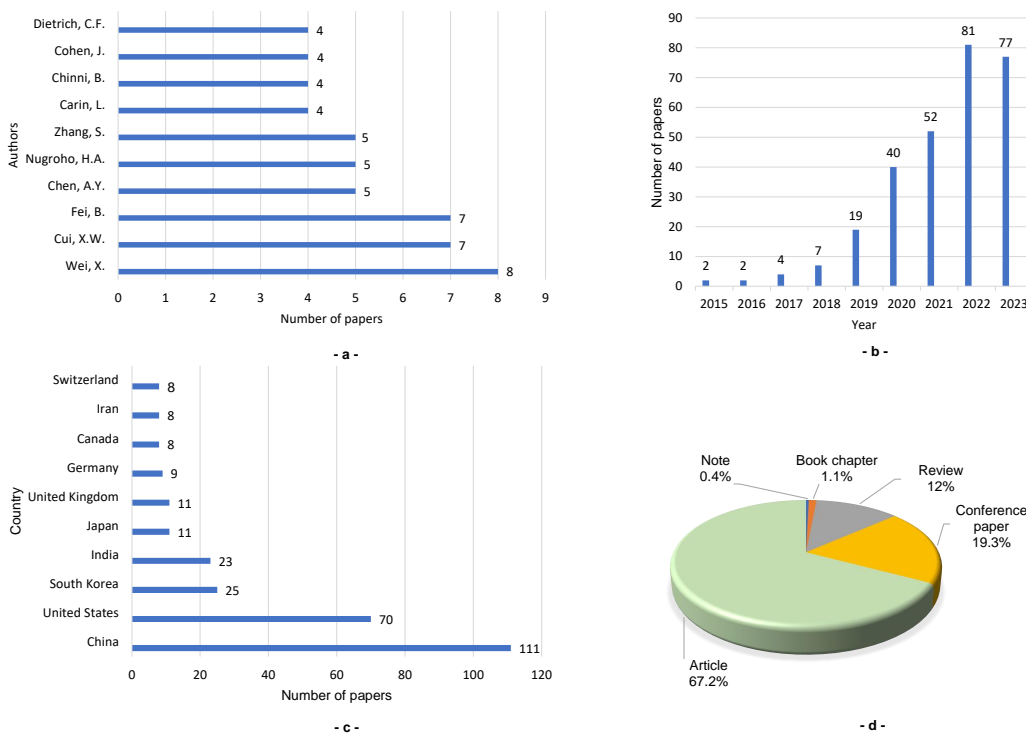


Figure 2. Bibliometric analysis in terms of: (a) documents by author; (b) documents by year; (c) documents by country; (d) documents by type.

1.3. Roadmap

The subsequent sections of this manuscript are organized as follows: Section 2 discusses standardized assessment criteria and commonly used thyroid cancer datasets, emphasizing the importance of metrics and dataset features for AI-driven analysis in TCD. Section 3 provides a summary of current AI-based models and methods for TCD, including classification, segmentation, and prediction frameworks. Section 4 explores advanced TCD methods leveraging ViT and LLM, focusing on their segmentation, classification, and prediction applications. Section 5 outlines the limitations and challenges of existing AI methodologies, highlighting gaps in accuracy, data variability, and model generalizability. Section 6 discusses future research directions, emphasizing innovative approaches to ad-

vance AI technologies in TCD. Finally, Section 7 presents the conclusion, synthesizing key insights and reaffirming the transformative potential of AI in medical diagnostics while offering perspectives for its integration into TCD practices.

2. Standardized assessment criteria and commonly used datasets

2.1. Metrics

In this segment, we explore the standard metrics commonly utilized for evaluating thyroid disease (TD) detection performance. These metrics act as critical benchmarks for measuring the success of methodologies, underscoring the significance of choosing the right metrics to assess ML models. A variety of DL metrics are used to determine the efficiency of the suggested method in identifying TD. It is important to note that certain metrics have been previously addressed in [36]. The other metrics, particularly designed for image processing applications in TD, are concisely outlined in Table 2.

2.2. Datasets for TC

In the context of TC research, numerous datasets have been developed to support the testing and validation of ML algorithms and models. This step is crucial, given the significant challenge of compiling these datasets within the endocrine ML field. Table 3 lists examples of publicly available TCDs.

Table 2. Summary of the metrics for classification and regression employed in assessing AI-driven methods for TCD.

	Metric	Mathematical formula	Description
Classification and Regression	Specificity	$\frac{T_N}{T_N + F_P} \cdot 100\%$	This metric represents the proportion of accurately predicted negative samples out of all the negative samples.
	Root mean square error (RMSE)	$\left(\sqrt{1 - (ER)^2} \right) \times SD$	This is the standard deviation of the predicted errors between the training and testing datasets, and a lower value indicates the classifier's excellence.
	JSI	$\frac{ A \cap B }{ A \cup B } = \frac{T_P}{T_P + F_P + F_N}$	Paul Jaccard introduced this method to measure both the similarity and diversity among samples.
	Volumetric overlap error (VOE)	$\frac{F_P + F_N}{T_P + F_P + F_N}$	Assess the likeness between the segmented area and the ground truth area. VOE quantifies the level of overlap between these two regions and is calculated as the ratio of the combined volume of the segmented and ground truth regions to the volume of their intersection.
	Mean absolute error (MAE)	$\frac{1}{N} \sum_{i=1}^N a_i - p_i $	This measure indicates the average of the disparities between the real values and the predicted values.
Statistical	Standard deviation (SD)	$\sqrt{\sum(x - \mu)^2 / N}$	It quantifies the degree of variability or spread within a dataset.
	Correlation (Corr)	$\frac{(\sum((x - \mu_x) \cdot (y - \mu_y)))}{(\sqrt{(\sum(x - \mu_x)^2)} \cdot \sqrt{(\sum(y - \mu_y)^2)})}$	It characterizes the extent of correlation or connection between two or more variables.
	mean reciprocal rank (MRR)	$\frac{1}{ Q } \sum_{i=1}^{ Q } \frac{1}{rank_i}$	The MRR is a statistical measure used to assess the average reciprocal rank of outcomes for a set of queries, as explained in [37]. Here, "rank _i " denotes the position at which the first relevant document appears for the i-th query.
	Kappa de Cohen	$k = \frac{\Pr(a) - \Pr(e)}{1 - \Pr(e)}$	This metric gauges the level of agreement between two assessors, considering chance as a baseline.
Computer vision	Peak signal to noise ratio (PSNR)	$10 \cdot \log_{10}((MAX_I^2) / MSE)$	It quantifies the proportion between the highest achievable signal power and the power of the noise that impacts the faithfulness of its portrayal.
	Visual information fidelity (VIF)	$\frac{\sum_j I(C^j; F^j / s^j)}{\sum_j I(C^j; E^j / s^j)}$	It assesses the excellence of a reconstructed or compressed image or video in relation to the original signal. This evaluation considers how much visual information is retained in the processed image or video, accounting for the image's spatial and frequency attributes.
	Normalized cross-correlation (NCC)	$\frac{\sum_{i=1}^M \sum_{j=1}^N (I(i,j) - \bar{R}(i,j))^2}{\sum_{i=1}^M \sum_{j=1}^N I(i,j)^2}$	Assess the likeness between two images (or videos) by subtracting the mean value from each signal and subsequently normalizing the signals by dividing them by their standard deviation. Finally, compute the cross-correlation between the two normalized signals.
	Structural content (SC)	$\frac{\sum_{i=1}^M \sum_{j=1}^N I(i,j)^2}{\sum_{i=1}^M \sum_{j=1}^N R(i,j)^2}$	An elevated structural content value indicates that the image possesses lower quality.
	Noise visibility function (NVF)	Normalization $\left\{ \frac{1}{1 + \delta_{bloc}^2} \right\}$	This calculates the texture information within the image, where δ_{bloc} represents the variance in luminance.

Table 2 (Continued)

Metric	Mathematical formula	Description
Visual signal to noise ratio (VSNR)	$10 \log_{10} \left(\frac{C^2(I)}{(VD)^2} \right)$	This approach sets distortion thresholds using contrast computations and wavelet transforms. VSNR is deemed excellent if distortions are below the threshold. It uses RMS contrast ($C(I)$) and visual distortion (VD).
Weighted signal-to-noise ratio (WSNR)	$10 \log_{10} \left(\frac{\sum_{u=0}^{M-1} \sum_{v=0}^{N-1} A(u,v)C(u,v) ^2}{\sum_{u=0}^{M-1} \sum_{v=0}^{N-1} A(u,v) - B(u,v)C(u,v) ^2} \right)$	It relies on the contrast sensitivity function, with $A(u,v)$, $B(u,v)$, and $C(u,v)$ denoting the 2D discrete Fourier transforms (TFD), as described in [38].
Normalized absolute error (NAE):	$\frac{\sum_{i=1}^M \sum_{j=1}^N I(i,j) - R(i,j) }{\sum_{i=1}^M \sum_{j=1}^N I(i,j) }$	This metric assesses the precision of an ML model's predictions by quantifying the discrepancy between predicted and actual values relative to the range of actual values.
Laplacian mean square error (LMSE)	$\frac{\sum_{i=1}^M \sum_{j=1}^N L(I(i,j)) - L(R(i,j)) ^2}{\sum_{i=1}^M \sum_{j=1}^N L(I(i,j)) ^2}$	It is a modified version of mean square error (MSE), utilizing the Laplacian distribution instead of the Gaussian distribution. $L(I(i,j))$ represents the Laplacian operator.

Table 3. Instances of publicly available TCDs utilized in the identification of TC.

Ref.	TCD	Description	Link
[39]	THO	This dataset is designed to investigate the fundamental causes and effects of TD through the application of diverse omics approaches, including genomics, epigenomics, transcriptomics, proteomics, and metabolomics.	Visit THO datasets
[40]	TDD	The dataset used for classification encompasses 5 features and 7200 instances, featuring a mix of 15 categorical and 6 numerical attributes. The classes within this dataset comprise hypothyroid, hyperfunction, and subnormal functioning.	Visit TDS datasets
[41]	KEEL	The KEEL dataset offers a collection of benchmarks for assessing the performance of different learning approaches, including semi-supervised classification and USL. It encompasses 21 features, 7200 instances, and 3 classes.	Visit KEEL datasets
[42]	GEO	The gene expression omnibus (GEO) database serves as a repository for genomics data. It is specifically structured to archive gene expression datasets, arrays, and sequences within GEO.	Visit GEO datasets
[43]	DDTI	The digital database thyroind image (DDTI) dataset acts as an essential tool for both researchers and novice radiologists aiming to create algorithm-driven CAD systems for analyzing TN. It contains 99 cases and 134 images.	Visit DDTI datasets
[44]	NCDR	The national cancer data repository (NCDR) functions as a repository for healthcare and research purposes, aimed at documenting every reported instance of cancer within England. The data originates from the Office for National Statistics.	Visit NCDR datasets
[45]	PLCO	The National Cancer Institute backs the prostate, lung, colorectal, and ovarian (PLCO) cancer screening trial, which focuses on identifying the primary factors influencing cancer incidence in both genders. This trial encompasses records from 155,000 participants and includes comprehensive studies on TC incidence and mortality.	Visit PLCO datasets

3. Summary of current models and methods

This section discusses the various AI-based methodologies utilized for diagnosing thyroid gland (TG) cancers. Figure 3 offers a visual depiction of the classification system for TC diagnosis methods leveraging AI.

3.1. Purpose of AI-driven examination

This review centres on the use of AI for identifying TC. Comprehending the foundational objectives of each framework is essential for acquiring a more profound understanding of their reasoning [8].

(a) Classification of thyroid carcinoma: Entails the sorting of TCs according to their histopathological features, clinical manifestations, and prognostic outcomes. Various forms of thyroid carcinomas exist, each defined by unique characteristics. The principal categories are: (i) PTC: Representing the most prevalent form, PTC constitutes approximately 80% of all TC cases. It typically exhibits slow growth but has a propensity to metastasize to neck lymph nodes. Nonetheless, PTC generally responds well to treatment. (ii) FTC: Ranking as the second most frequent type, FTC has the capability to invade blood vessels and spread to distant body parts, although it is less prone to lymph node metastasis. (iii) MTC: Arising from the parafollicular or C cells of the thyroid, which secrete calcitonin, an increase in blood calcitonin levels may signal MTC. (iv) ATC: ATC is a highly aggressive and rare TC variant, characterized by its rapid spread to other neck regions and the body, making it challenging to treat. The stratification of thyroid carcinomas is vital for selecting the optimal treatment plan for individual patients, considering tumour dimensions, location, patient

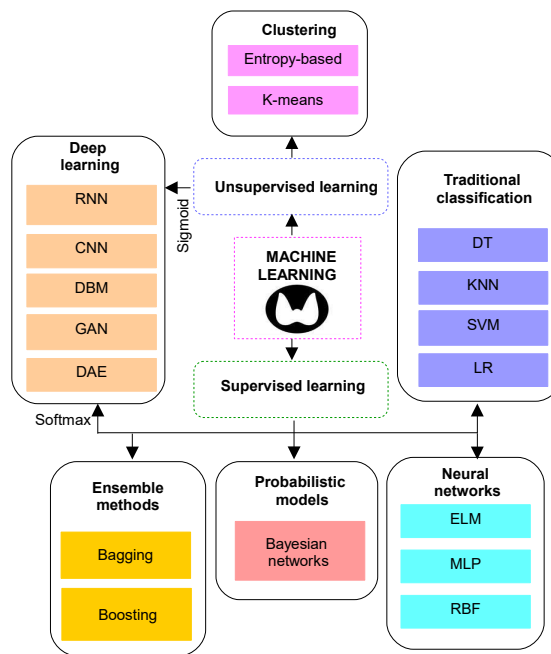


Figure 3. Classification of TCD strategies utilizing AI.

age, and general health. The evolution of AI and ML has significantly contributed to the automation and enhancement of thyroid carcinoma classification accuracy. Various models have been devised to categorize tumours based on medical imaging or genetic information. For example, Liu and colleagues [46] highlight the fundamental importance of support vector machine (SVM) in the detection of cancer. In a similar vein, Zhang and their team [47,48] introduce approaches utilizing deep neural network (DNN) to distinguish between malignant and benign TNs in US imagery. Moreover, the bi-directional LSTM (Bi-LSTM) model [49], shows noteworthy precision in the classification of TNs. These classification approaches create structured hierarchies crucial for organizing knowledge and processes in the field of TCD.

(b) Segmentation of thyroid carcinoma: Segmentation plays a pivotal role in the detection of TC by enabling the accurate isolation and analysis of the thyroid gland, along with any potentially suspicious nodules or lesions present [50]. Often detected through medical imaging modalities like US, computed tomography (CT) scans, or magnetic resonance imaging (MRI), TCD requires the precise delineation of the region of interest (ROI) for sound diagnostic judgements. Segmentation not only facilitates the distinction of the thyroid gland from the surrounding tissues but also supports the precise quantification of nodule dimensions and volume, which are critical for evaluating the potential for malignancy. Furthermore, it enables the extraction of significant image attributes such as texture and shape, providing critical data for ML models or other analytical methods to improve diagnostic precision. Segmented images also enhance visual clarity, aiding radiologists and medical practitioners in the visual assessment and interpretation of areas of concern within the thyroid, vital for detecting abnormalities indicative of cancer. For longitudinal analyses, segmentation is invaluable in tracking changes in the thyroid and nodules over time, monitoring disease evolution or the efficacy of treatments. It also plays a role in accurately locating biopsy sites for suspicious nodules, guaranteeing targeted sample collection for cancer verification. In the context of treatment planning, segmentation is instrumental in assessing the tumour's size and its relationship to vital anatomical structures, thereby guiding therapeutic decisions. Moreover, the introduction of automated segmentation technologies streamlines clinical workflows by minimizing manual input and variability, empowering medical experts to dedicate more attention to complex diagnostic activities. Consequently, the segmentation process in TCD enhances precision, consistency,

and confidence in diagnostics, markedly impacting patient management and outcomes. AI methods, especially convolutional neural network (CNN) and the U-Net architecture, are becoming progressively popular for the segmentation of thyroid carcinoma. Their growing preference is largely due to their capacity to learn from and generalize across large datasets, significantly improving the accuracy and dependability of the segmentation procedure.

(c) Prediction of thyroid carcinoma: Prediction in TCD involves utilizing diagnostic tools and ML models to estimate the risk of development based on factors like genetic predisposition, gender, age, radiation exposure, and lifestyle choices. It's important to note that predictions indicate a heightened risk rather than a definite outcome. Medical practices often combine various predictive assessments to improve accuracy. For example, ML algorithms developed from medical records can help distinguish between benign and malignant nodules, facilitating early intervention. Studies, such as one utilizing artificial neural network (ANN) and logistic regression (LR), and another employing a CNN to analyze over 10,000 microscopic TCD (images) [51], demonstrate the application of predictive techniques in identifying TC risk, showcasing advancements in AI-driven predictive modelling for more effective treatment strategies.

3.2. *Pre-processing*

Principal component analysis (PCA) operates as a sophisticated method for pre-processing, transforming samples (variables) into a smaller set of uncorrelated ones. This technique effectively reduces the volume of variables, thus cutting down on redundant data, all the while striving to maintain the integrity of the data relationships. PCA is extensively used in the realms of cancer detection and distinguishing between malignant and benign thyroid cells. In research conducted by Shankarlal et al. [52], PCA was deployed to filter the most relevant set of wavelet coefficients from double-tree complex wavelet transform (DTCW) processed noisy thyroid images, which were then categorized using random forest (RF). In another instance, Soulaymani et al. [53] applied PCA to a dataset comprising 399 patients with three different TC, allowing the classification based on variables like age, sex, type of cancer, and geographical location.

3.3. *ML features selection and extraction*

3.3.1. Selection methods

The primary goal of the selection process is to identify and select relevant features that can enhance the accuracy of classification, simultaneously eliminating non-essential variables [54]. Many techniques of feature selection are proposed:

(a) Correlation-based feature selection (CFS): The CFS technique is commonly applied to examine the relationships between various cancer-related attributes. Although CFS offers a range of advantages, there are also notable limitations associated with its use in feature selection within ML:

- **Advantages:** CFS is valued for its straightforwardness, ability to identify linear correlations, capability to decrease dimensionality, and potential to boost model efficiency and clarity. This method supports quicker model training and prediction, exhibits robustness against outliers, and accommodates the incorporation of expert insights. Moreover, it enhances the effectiveness of other methodologies, provides opportunities for visualization and deeper understanding, lowers expenses, and enables the conduct of sensitivity analyses.
- **Disadvantages:** It's important to recognize that this approach may miss complex, nonlinear relationships between features and the outcome variable. Additionally, it can be vulnerable to multicollinearity, where features are highly correlated with each other, requiring additional preprocessing steps. Careful consideration of the specific issue and dataset at hand is crucial when applying this method.

The CFS algorithm has been widely incorporated into feature selection strategies to enhance classification outcomes across various studies. For example, in [55], researchers utilized CFS for feature selection within microarray datasets, successfully minimizing data

dimensionality and pinpointing significant genes. A combined model that blended CFS with binary particle swarm optimisation was developed in [56] for cancer classification, and applied to 11 standard microarray datasets. Additionally, the CSVM-RFE technique, which integrates CFS, was applied in [57] to diminish the feature set in cancer research by removing non-essential elements. Moreover, CFS methodologies were utilized in [58] for the identification of key RNA expression features.

(b) Relevance analysis: The relevance analysis (RA) is an effective technique used in feature selection, evaluating the discriminative power of features between classes through score assignment. RA has its own array of advantages and disadvantages:

- **Advantages:** RA offers several benefits in feature selection, including its robustness against noisy data, capability to handle both continuous and categorical features, and ability to detect feature interactions without assuming their independence. It also reduces bias in datasets with imbalanced classes, eliminates the need for model training, and facilitates sensitivity analysis. These attributes make RA an advantageous tool for feature selection in various data scenarios.
- **Disadvantages:** RA exhibits significant computational complexity, affecting its applicability to large datasets. Its performance is sensitive to parameters, particularly the choice of the number of nearest neighbours (k), which can be challenging to optimize. The stability of RA is also affected, with variations in the dataset leading to different selections of features. Furthermore, it is designed solely for use within SL contexts, struggles with non-metric features, and necessitates adaptations for handling multiclass classification scenarios.

This method evaluates the importance of different features by exploring the relationships between variables related to cancer. In their research, Cui et al. [54] suggested a feature selection strategy that employs the RA algorithm to enhance its effectiveness.

3.3.2. Extraction methods

(a) PCA: Principal component analysis (PCA) has been widely recognized in numerous pieces of research for its effectiveness in reducing data dimensionality and decoupling cancer-related features. PCA is praised for its ability to decrease dimensions and reveal patterns, although it may compromise on interpretability and is optimally used with linear correlations. For example, Shankarla et al. (2020) implemented PCA to refine feature selection for TCD via the DTCW transformation [52]. Soulaymani et al. (2018) investigated PCA's capability in distinguishing various TC subtypes, such as papillary, follicular, and undifferentiated types [53]. Additionally, O et al. (2019) assessed PCA and linear discriminant analysis in the classification of Raman spectra for different TC subtypes [59].

(b) Texture description: Texture analysis is a highly regarded technique for extracting related data in TC segmentation, classification, and prognosis efforts. The scientific community has developed various texture analysis methods, including wavelet transforms, binary descriptors, and statistical descriptors, among others. Specifically, the discrete wavelet transform (DWT) has garnered significant interest for its exceptional capability in data decorrelation. Although texture analysis is beneficial for distinguishing textures, it can be affected by changes in lighting conditions and does not inherently understand semantic content, which may limit its application in complex visual tasks. Wavelet-based methods have been extensively applied in detecting TC. For example, Sudarshan et al. [60] applied wavelet techniques to identify cancerous areas in thyroid, breast, ovarian, and prostate tumours. Additionally, Haji et al. [61] used texture data for the diagnosis of TN malignancy employing a 2-level 2D wavelet transform. Further contributions to this field are documented in studies such as [62] and [63].

(c) Active contour (AC): The AC model, a versatile framework often used in image processing, was initially introduced by Kass and Witkin in 1987. AC is known for its ability to adjust to complex shapes, yet it faces challenges such as sensitivity to initial placements

and issues with overlapping figures. Various strategies have been developed to address these challenges in contour segmentation using deformable curve models. These models have seen significant application in TCD, as evidenced by research conducted by [64], [65], and [66].

(d) LBP and GLCM: Local binary patterns (LBP) are descriptors used in computer vision for identifying textures or objects in digital images. They are appreciated for their straightforwardness and ability to distinguish features effectively. However, LBP may be vulnerable to noise and often requires tuning of parameters for optimal performance. The LBP method was employed in TCD, as illustrated in a study by Yu et al. [62]. Furthermore, the integration of LBP with DL has been explored for distinguishing between benign and malignant TN, as seen in the studies by Xie et al. [67] and Mei et al. [68].

The gray-level co-occurrence matrix (GLCM) serves as a tool to depict the occurrence frequency of pixel value pairs at a predetermined distance within an image. It is particularly useful for texture analysis and the identification of distinctive features. Nevertheless, GLCM faces challenges such as sensitivity to image variations, high computational demands, and the need for careful parameter tuning. For example, Dinvicic et al. [69] employed GLCM in a comparative study to investigate the differences between patients with Hashimoto's thyroiditis-associated PTC and those with Hashimoto's thyroiditis only.

(e) ICA: In independent component analysis (ICA), data is decomposed into a set of independent contributing features to aid in feature extraction. ICA is adept at identifying statistically independent components, making it valuable for tasks like source separation. Its strengths lie in uncovering non-linear relationships and facilitating data compression. Nonetheless, ICA faces challenges due to assumptions about the data mixing process and can be difficult to interpret. ICA is applied for disentangling multivariate signals into their separate constituents. In the research conducted by Kalaimani et al. [70], ICA was used to isolate 29 attributes as independent and significant features for categorizing data into hypothyroid or hyperthyroid groups through a SVM. A portrayal of the techniques derived from ML/DL utilized in diagnosing TC is provided in Table 4.

Table 4. Summary of features methods based on ML/DL conducted in the diagnosis of TC.

Ref.	Year	ML/DL	Classifier	Features	Contributions
[71]	2017	ML	KNN	FC/IG	Minimize data duplication and decrease processing duration. KNN addresses absent dataset values, while ANFIS receives the modified data as input.
[72]	2017	ML	SVM	FC/CFS	Retrieve the geometric and moment characteristics, while specific SVM classifier kernels categorize the acquired features.
[73]	2020	DL	CNN	FC/R	Utilize both ML techniques and feature selection algorithms, specifically Fisher's discriminant ratio, Kruskal-Wallis analysis, and Relief-F, for the examination of the SEER database.
[74]	2022	DL	CNN	FE/PCA	This study mitigated the impact of imbalanced serum Raman data on prediction outcomes by employing an oversampling technique. Subsequently, the dimension of the data was reduced with PCA before applying RF and the Adaptive Boosting for classification.
[75]	2012	ML	Boosting	FE/TD	Integrate CAD with DWT and extract texture features. Utilize the AdaBoost classifier to classify images into either malignant or benign thyroid images based on the extracted features.
[76]	2021	DL	CNN	FE/AC	Improve image quality, perform segmentation and extract multiple features, including both geometric and texture features. Each feature set is subsequently classified using MLP and SVM, leading to the classification of either malignant or benign cases.
[77]	2020	ML	SVM	FE/LBP	Deep features are obtained through CNN, and they are merged with manually crafted features, which include histogram of oriented gradient (HOG) and scale-invariant feature transforms, to generate combined features. These combined features are subsequently employed for classification via an SVM.
[78]	2019	ML	SVM	FE/GLCM	Apply a median filter to mitigate noise and outline the contours before feature extraction from thyroid regions, encompassing GLCM texture features. Subsequently, employ SVM, RF, and Bootstrap Aggregating (Bagging) to differentiate between benign and malignant nodules.
[70]	2019	ML	SVM	FE/ICA	A multi-kernel-based classifier is employed for thyroid disease classification.

3.4. SL-based TCD classification

SL provides high accuracy, interpretability, and robust predictive capabilities. However, it necessitates extensive labeled data, poses risks of overfitting, and can be computationally intensive [79]. The following algorithms represent prominent SL techniques utilized in TCD:

(a) DT and LR: Decision tree (DT) learning is a technique in data mining that uses a model for predictive decision-making. In such a model, the outcomes are indicated by the leaves, and the branches represent the input features. This method has been utilized in detecting latent thyroid disorders, as evidenced by a range of studies, such as in [80]. In the research presented in [81], LR was employed to pinpoint specific characteristics of thyroid microcarcinoma among a group of 63 patients. This analysis utilized data from both contrast-enhanced ultrasound (CEUS) and traditional US evaluations. Furthermore, a significant study from northern Iran, detailed in [82], used LR to investigate a large dataset encompassing 33,530 cases of TCD. LR is a widely used binomial regression model within the domain of ML.

(b) ELM and MLP: The extreme learning machine (ELM) model is distinguished by a single layer of hidden nodes that possess randomly assigned weight distributions. Crucially, the process of determining weights between the inputs and the hidden nodes to the outputs is executed in a solitary step, rendering the learning mechanism markedly more efficient than that of alternative models. The efficacy of the ELM approach in diagnosing TD has been corroborated through various research efforts [83].

The multilayer perceptron (MLP) is a type of feed-forward network that directs data processing sequentially from the initial point to the final layer of output. Within this architecture, each layer is made up of a different number of neurons. Rao and colleagues [84] devised an innovative approach for categorizing TNs employing an MLP integrated with a backpropagation learning mechanism. Their design comprised four neurons in the initial layer, three neurons in each of its ten concealed layers, and one neuron in the terminal layer. In a separate effort to enhance the precision of TD diagnosis, Hosseinzadeh et al. [85] utilized MLP networks. Their analysis compared the efficacy of MLP networks against the backdrop of existing research on TCD classification, highlighting the superior performance of MLP networks.

(c) PM and EM: probabilistic modelss (PMs), such as Bayesian networks, are vital in computer science and statistics for modeling uncertainties and variable dependencies. They support decision-making in ML, data analysis, and parameter estimation. Bayesian networks use directed acyclic graphs, aiding in reasoning under uncertainty, predictions, and medical diagnosis of TNs. In the realm of oncology research, tackling the intricacies of cancer datasets and enhancing the accuracy of detection frequently involves the use of EMs. This strategy splits the dataset into several subsets, upon which a variety of ML algorithms are applied in parallel. The insights gained from these individual algorithms are subsequently merged to derive a comprehensive diagnosis. The main goal behind adopting EMs is to forge a superior predictive model tailored for the detection of TC. Such an approach has been validated in multiple studies, including a significant one conducted by Chandran et al. [86], where the authors underscored the contribution of EMs to a more profound data comprehension and heightened diagnostic accuracy.

(d) Bagging and Boosting: Bagging is a notable ensemble learning approach in TCD, aimed at boosting the accuracy and consistency of ML algorithms. This technique achieves its objectives by lowering variance and offering protection against overfitting. It finds broad application in a variety of methods, with a particular emphasis on DT. The main goal of Bagging is to improve the effectiveness of weaker classifiers in the context of TCD screening. In their research, Chen et al. [87] presented feature bagging (FB) as an ensemble learning strategy designed to reduce the correlation between models in an ensemble. FB accomplishes this by training each model on randomly selected feature subsets from the dataset, rather than using the full set of features. The utility of FB is demonstrated in its ability to distinguish between benign and malignant cases of TC [88]. Within the scope of USL, meta-algorithms play a crucial role in reducing variance and improving the performance of weak classifiers, effectively converting them into robust classifiers [89].

In the context of boosting, Pan et al. in their study [90] employed a novel method called AdaBoost to identify TN, utilizing the widely recognized university of California,

Irvine (UCI) dataset. The classification was performed using the random forest method, with PCA employed to retain data variance. Chen et al. [91], the gradient tree boosting (XGBoost) algorithm was highlighted as a powerful implementation of gradient-boosted DT, with its application extending across multiple research areas including sports and health monitoring [92]. Specifically, in the context of TC, the XGBoost algorithm was employed by researchers to distinguish between benign and malignant TN [93], offering a solution to the problem of obtaining accurate diagnoses without the need for large datasets that DL models usually require.

3.5. USL-based TCD classification

USL is the process of analyzing data that hasn't been previously labelled or annotated. Its primary goal is to uncover the underlying structures within datasets that do not have predefined labels. Contrary to SL, which depends on labelled data for evaluating its effectiveness, USL operates without such direct guidance, presenting additional challenges in result assessment. Although USL algorithms are capable of addressing more complex problems than their supervised counterparts, they might also lead to increased uncertainty, sometimes creating unintended categories or incorporating noise rather than identifying clear patterns. Nonetheless, USL is considered an indispensable asset in AI, offering the potential to detect patterns within data that may not be obvious at first [94].

Clustering is one of the important techniques in USL. The objective of this strategy is to organize TCD into distinct, uniform groups that share similar features. This process aids in the categorization of unlabeled data into malignant or benign sections. Due to its straightforwardness, this technique has received significant attention in numerous medical research areas, enhancing its applicability to tasks like identifying breast cancer [95], and discovering brain tumours [96]. Clustering methods also prove helpful in classifying cancer instances that are not clearly defined [97]. A research documented in [98] employed clustering to determine factors impacting the normal functioning of the thyroid gland. The use of PCA played a key role in organizing the clusters and simplifying the data structure. Additionally, an innovative automated clustering system for diagnosing TC was developed, as described in [99], which recommended appropriate medication treatments for hyperthyroidism, hypothyroidism, and normal cases. As an example, the study in [100] explored the use of fuzzy clustering on thyroid and liver datasets from the UCI repository, where fuzzy c-means (FCM) and possibilistic fuzzy c-means (PFCM) algorithms were employed and their performances compared.

(a) K-means (KM): The KM method is used for dividing data into partitions and tackles a combinatorial optimization challenge. It is commonly used in USL, categorizing observations into k distinct clusters. In the research presented by Mahurkar et al. [101], the study investigates the application of ANN and an improved K-Means algorithm to standardize raw data. This study employed a thyroid dataset from the UCI repository, comprising 215 total instances.

(b) Entropy-based (EB): In the study conducted by Yang et al. [102], a novel, parameter-free computational model called DeMine was introduced for the prediction of microRNA regulatory modules (MRMs). DeMine utilizes an information entropy-based methodology, comprising three primary steps. The process begins by converting the miRNA regulation network into a cooperative MRMs network. It then proceeds to pinpoint miRNA clusters, aiming to maximize entropy density within the specified cluster. The final step involves grouping co-regulated miRNAs into their appropriate clusters, thereby finalizing the MRMs. This technique enhances predictive precision and facilitates the identification of a broader array of miRNAs, potentially acting as tumour markers in cancer diagnosis.

3.6. DL-based TCD classification

DL surpasses traditional ML by automating feature extraction, enhancing performance with large datasets, and offering scalability for complex models. Table 5 presents a com-

parison between ML and DL in the context of TCD. Key methods for TCD include CNNs for image analysis, recurrent neural networks (RNNs) for sequential data, transfer learning (TL) for leveraging pre-trained models [103], ensemble learning for robustness, and attention mechanisms for focused detection. These advancements enable more accurate and efficient early detection, improving patient outcomes.

Table 5. Comparison of ML and DL for TCD.

Criteria	DL	ML
Best Suitable Scenario	Large datasets with complex features relevant to thyroid cancer characteristics	Smaller datasets with simpler features, suitable for initial screening
Advantages	<ul style="list-style-type: none"> High accuracy with large, diverse data Automated feature extraction from complex medical images and data Capable of identifying subtle patterns indicative of thyroid cancer 	<ul style="list-style-type: none"> Effective with smaller datasets, reducing the need for extensive data collection Easier interpretation and understanding of models by medical professionals Faster training times suitable for rapid decision-making in clinical settings
Disadvantages	<ul style="list-style-type: none"> Requires large labelled datasets for training, which can be challenging to acquire and annotate Computationally intensive, requiring high-performance hardware and longer processing times 	<ul style="list-style-type: none"> Requires manual feature engineering to extract relevant medical features Limited performance in capturing intricate patterns or anomalies in complex thyroid conditions
Performance	Excels in analyzing high-dimensional medical imaging data	Performs well with structured clinical data from standard medical tests
Resource Requirements	High (GPUs, memory, computational power) due to complex data processing	Moderate (CPUs, less memory) sufficient for structured data analysis
Risk of Overfitting	High, mitigated with regularization techniques and extensive validation	Moderate, mitigated with cross-validation strategies
Future Development	Integration with advanced USL for discovering new disease markers and improved annotation techniques	Enhanced algorithms for feature selection and hybrid models combining DL's imaging capabilities with ML's interpretability

Typically, the network's depth facilitates the extraction of increasingly abstract and advanced features as data moves through its layers. By leveraging large neural networks with several layers, DL can independently learn, create, and improve data representations, which is why it is known as "deep" learning. Within the realm of TCD, DL is instrumental in several areas, including: (i) Classification of image: DL techniques, for example CNN, are trained to categorize thyroid US images, distinguishing between malignant and benign nodules by analyzing texture and shape, and other features [104,105], streamlining the process and assisting with the early identification of TC; (ii) Analysis of disease: DL is used to examine cytopathological or histopathological slide images, aiding in identifying and classifying cells of cancerous; (iii) Analysis of genomic information: In this era DL models are capable of analyzing genetic variations linked to the risk of TC; (iv) Radiomics: DL models are adept at extracting multidimensional information obtained from radiographic images, contributing to more accurate and individualized treatment strategies; and (v) Predictive analysis: By analyzing electronic health records and patient information, DL models can forecast the probability of an individual developing TC, facilitating early intervention. The following DL algorithms are the widely used techniques for TCD:

(a) DAE: Denoising autoencoders (DAEs) play a pivotal role in the identification of TC by adeptly deriving significant features from US or histopathological imagery. As a subset of ANN, DAE are primarily focused on the accurate reconstruction of inputted data. Their usage extends to tasks such as reducing dimensions and enhancing feature learning capabilities. The integration of DAEs into the workflow for classifying thyroid carcinoma typically unfolds in several phases: (i) initial data pre-processing, (ii) creation of perturbed input data, (iii) training the DAE, (iv) extraction of relevant features, and (v) execution of the classification procedure. In the research presented by Ferreira et al. [106], a variety of six autoencoder models were utilized for the purpose of classifying PTC, incorporating strategies such as the stabilization of weights and network fine-tuning. The architecture of these autoencoders, especially the encoding layers, played an integral role in the effective integration of the network. In a related study by Teixeira et al. [107], both DAEs and their

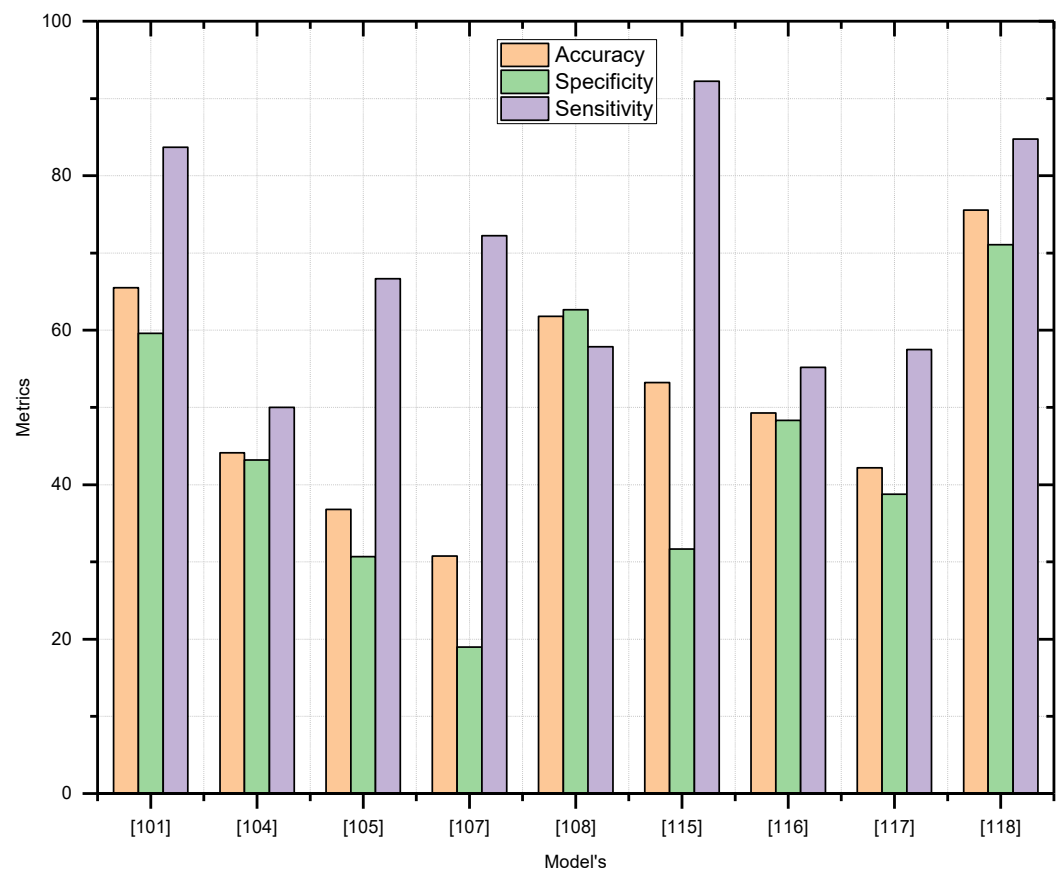


Figure 4. Synopsis of CNN-driven research in TC diagnosis with percentages for accuracy, sensitivity, and specificity [101], and [104,105,107,108,115–118].

stacked configurations were applied to distill crucial features and pinpoint genes relevant to TC diagnosis.

(b) CNN and RNN: CNNs, a branch of DL models, stand out for their remarkable capabilities in tasks such as image analysis and processing, including the classification of medical images. Their efficiency in managing data structured in grids, like images where the spatial relationship between pixels is crucial, makes them particularly suited for these tasks. The focus on CNN-based techniques for TCD, especially in automating nodule identification and classification in US imagery [108], has grown significantly. The ConvNet model, known for its reliance on convolution operations vital for image recognition tasks [109], is a prime example of this effort. Various architectures of CNN such as VGG, AlexNet, and GoogleNet, among other [110], are celebrated for their inclusion of convolutional, pooling, and fully connected layers. In a notable study by Li et al. [111], the efficacy of CNN models in predicting TC was investigated, utilizing a dataset of 131,731 US images from 17,627 patients. Xie et al. [112] implemented models such as Inception-Resnet, Inception, and VGG16 to differentiate malignant from benign tissues in 451 images of thyroid from the DDTI dataset, employing image augmentation to mitigate data limitations prior to classification. Moreover, Koh et al. [113] assessed the diagnostic accuracy of deep convolutional neural network (DCNN) models against that of expert radiologists for identifying TNs in US images, using a dataset of 15,375 images and showcasing the CNNE1 and CNNE2 models derived from DCNN for differentiating between malignant and benign nodules. Liang et al. [114] introduced a DL based on CNN for classifying and detecting thyroid and nodules of breast, comparing its performance with traditional US imaging results. Figure 4 depicts the recent advancements in classifying TCD via CNN-based methods.

RNNs characterized by connections between units forming a directed graph across temporal sequences. This structure allows them to leverage internal memory, making them adept at handling inputs of varying lengths. Consequently, RNNs excel in tasks that require understanding temporal dependencies, such as speech recognition, language translation, and time-series analysis. Within the realm of thyroid carcinoma classification, RNNs offer promising capabilities for analyzing data that is sequential or time-sensitive. This includes observing the evolution of clinical symptoms over time, tracking changes in tumours using successive medical images, or studying fluctuations in gene expression associated with the onset of TC. For example, Chen et al. (2017) utilized a hierarchical RNN structure to categorize TNs by analyzing historical US reports [119]. Their model comprises three layers of long-short-term-memory (LSTM) networks trained independently. The findings from their study suggest that this hierarchical RNN approach surpasses conventional models such as SVM + Unigrams, SVM + Bigrams, CNN, and LSTM in accuracy, computational efficiency, and robustness. These benefits are attributed to the RNN's memory mechanisms, which permit the retention of information from previous states through feedback loops, thereby making RNNs highly effective for cancer detection applications.

(c) GAN: Generative adversarial network (GAN) is composed of two key elements: a generator and a discriminator. The generator's function is to convert a random input vector into a data point that fits within the space of the dataset. Conversely, the discriminator serves as a binary classifier, tasked with assessing whether input data, originating either from the training dataset or produced by the generator, is genuine. GANs have found extensive applications in medical diagnosis, notably in the detection of TN [120].

Table 6 serves as an overview of various research initiatives aimed at identifying both benign and malignant forms of TC. It outlines the classifiers used, diseases focused on, datasets applied, research goals, and metrics for assessment. This table helps categorize the AI techniques applied in TCD, underlining their key roles in the domain.

3.7. Comparative analysis and discussion

This section commits to an exhaustive examination of AI models' proficiency in identifying thyroid carcinoma. We aim to scrutinize not merely their statistical precision but also their efficacy in practical clinical environments, and their contribution to the overarching clinical decision-making framework. Furthermore, this exploration delves into the potential biases embedded in AI models, seeking to unveil how they might inadvertently amplify existing healthcare inequities. By contrasting AI-enabled methodologies with conventional diagnostic tactics, we aspire to glean deeper insights into their relative effectiveness.

The reported metrics of AI models, such as accuracy, sensitivity, and specificity, can vary significantly across academic publications due to factors like the choice of dataset, data quality, and the methodological approach utilized. The performance of AI models in controlled experimental setups may not accurately represent their effectiveness in actual clinical scenarios. Variables including data discrepancies, lack of complete data, and evolving clinical conditions can substantially influence outcomes. Therefore, assessing a model's flexibility and reliability in diverse conditions is crucial. Table 7 provides an overview of the performance indicators for various AI-enhanced TCD frameworks, presented in percentage (%) terms, across multiple models and data sources. Additionally, Figures 5 and 6 display these performance indicators, also in percentage (%) terms, with a focus on private datasets and US imaging data, respectively.

3.8. Case study example

To exemplify the approaches adopted in the literature for TCD and the utilization of AI in classifying cancer types, we provide a simplified example. The pattern recognition process entails training a neural network to accurately classify input patterns into specific target classes. Following training, the network becomes capable of categorizing model. In this part, we demonstrate an example of categorizing TC into benign, malignant, or normal based on a collection of characteristics according to the TIRADS.

Table 6. Summary of studies on identifying benign and malignant TC, sorted by reference.

Ref.	AI Tech.		Classifier			Objective	DD	Dataset	APP	SV
	ML	DL	CNN	SVM	ELM					
[51]	✓	✓	✓			C	TC	PD	Omics	10068 images
[53]	✓	✓			✓	C	TC	PD	NA	NA
[58]	✓		✓			C	PTC	TCGA	Omics	500 patients
[80]	✓				✓	C	TC	UCI	US	3739 patients
[81]	✓				✓	C	TC	PD	US	63 patients
[82]	✓				✓	C	TN	PD	US	33,530 patients
[84]	✓				✓	C	TD	PD	US	7200 samples
[85]	✓				✓	C	TD	UCI	US	7200 patients
[87]		✓			✓	C	TN	PD	US	1480 patients
[101]	✓				✓	C	TC	UCI	US	215 instances
[102]	✓				✓	C	TC	PD	US	734 cases
[106]		✓			✓	C	PTC	TCGA	US	18985 features
[107]		✓			✓	C	PTC	TCGA	Omics	510 samples
[111]		✓	✓			C	TC	PD	US	1762 patients
[112]		✓	✓			C	TC	PD	US	1110 images
[114]		✓	✓			C,P	TN	PD	US	537 images
[119]		✓			✓	C	TN	PD	US	13592 patients
[121]	✓				✓	C	TD	PD	US	7200 instances
[122]	✓				✓	C	TD	UCI	US	215 patients
[123]	✓				✓	C	TD	PD	US	187 patients
[124]	✓				✓	C	TC	NA	US	NA
[125]	✓				✓	C	TC	UCI	US	499 patients
[126]		✓	✓			C	TC	PD	Omics	482 images
[127]		✓	✓			NA	PTC, FTC	NA	FNAB	NA
[128]		✓	✓			C	PTC	PD	FNAB	370 MPG
[129]		✓	✓			P	PTC	PD	FNAB	469 patients
[130]		✓	✓			C	TC	DDTI	US	298 patients
[131]		✓	✓			C	TC	PD	US	1037 images
[132]		✓	✓			P	TN	PD	US	80 patients
[133]		✓	✓			P	TN	PD	US	300 images
[134]		✓	✓			C	TC	PD	US	459 labeled
[135]		✓	✓			C	TD	ImageNet	US	2888 samples
[136]		✓			✓	NA	TC	NA	US	NA
[137]		✓			✓	C	TC	PD	US	1358 images
[138]	✓				✓	C	TC	PD	Surgery	50 patients
[139]	✓				✓	C	TC	PD	US	89 patients
[140]	✓				✓	C	TD	PD	Cyt	447 patients
[141]	✓	✓	✓		✓	C	FTC	PD	FNAB	57 smears
[142]	✓	✓	✓		✓	NA	FTC	NA	FNAB	NA
[143]	✓	✓	✓		✓	P	TC	TCGA	Hist	482 samples
[144]	✓	✓	✓		✓	C	TC	PD	FNAB	1264 patients
[145]	✓	✓	✓		✓	C	TN	PD	US	276 patients
[146]	✓				✓	C,P	FTC	PD	Hist	94 patients
[147]	✓				✓	C	TN	PD	US	467 TN
[148]		✓			✓	PTC	TCGA	Omics	115 slides	NA
[149]	✓				✓	C	TN	PD	Omics	121 patients

Abbreviation: Application (APP), Detected disease (DD), Subjects for validation (SV), Private data (PD), Classification (C), Prediction (P), Segmentation (S), Cytopathological (Cyt), Histopathological (Hist), Microphotographs (MPG).

The dataset obtained from the UCI ML repository has been used [180], which categorizes patients visiting a clinic into three distinct groups: normal, hyperfunctioning, or subnormally functioning. The dataset is structured into thyroid targets (TT) and thyroid inputs (TI) as detailed below: (i) TI consists of a $21 \times 7,200$ matrix that describes 7,200 patients through 15 binary and 6 continuous attributes. (ii) TT is a $3 \times 7,200$ matrix with class vectors, distributing each patient input into one of the three categories: (1) Hyperfunctioning, (2) Normal, not suffering from hyperthyroidism, and (3) Subnormal functioning.

In this neural network setup, the dataset is divided into 5,040 samples for training, 1,080 samples for validation, and 1,080 samples for testing purposes. The network undergoes training to minimize the error between the thyroid inputs and targets until it achieves the desired target objective. If the error rate (ER) fails to decrease and training progress stalls, training with the training data is stopped, and the validation data is utilized for additional evaluation. Subsequently, the testing data is employed to assess the accuracy of the trained model.

Figure 7 illustrates an instance of thyroid segmentation in US images utilizing k-means clustering, with three clusters selected for demonstration. K-means clustering is widely employed for such purposes. In this illustration, a network featuring 10 hidden layer neurons has been employed, 21 input features, and 3 output classes. Following the model

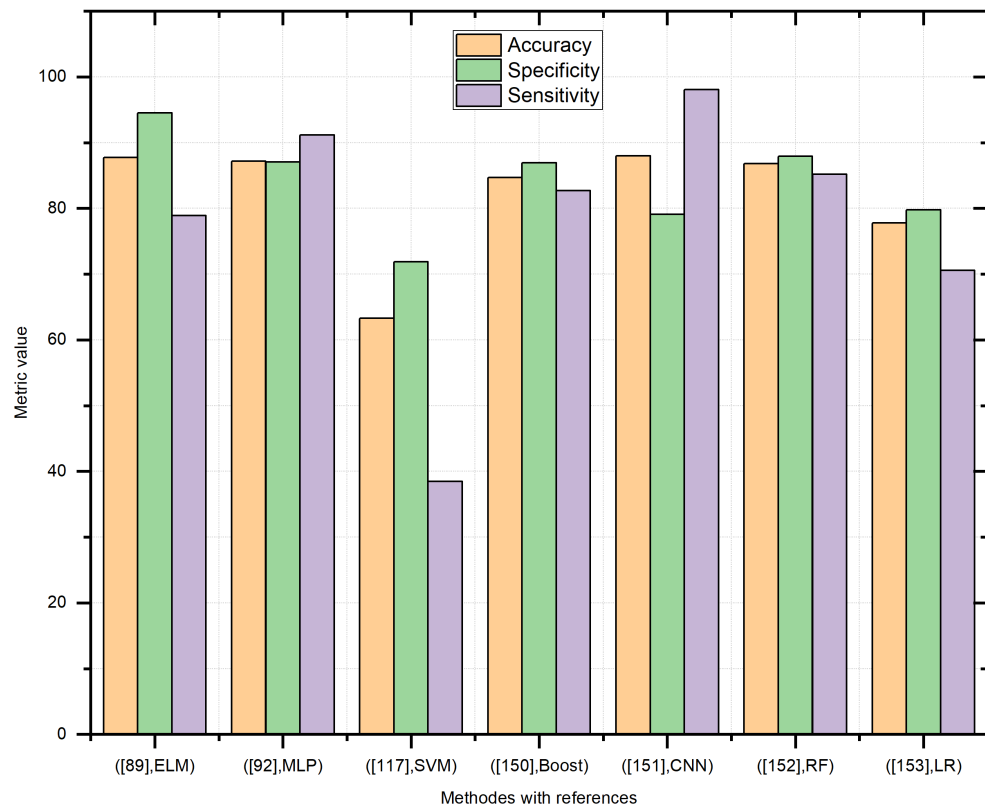


Figure 5. Performance assessment of TC frameworks in percentages (%) for private TCD [89], [92], [117], [150], [151–153].

Table 7. Assessment of the effectiveness of different TCD classification schemes, measured in percentages (%).

Ref.	AI Model	Dataset	SEN	SPE	ACC	AUC
[25]	RF	US	-	-	-	94.00
[105]	ThyNet	PD	-	-	-	92.10
[111]	DCNN	SGI	93.00	86.00	89.00	-
[115]	VGG-16	CI	-	-	97.66	-
[147]	DNN	ACR T	-	-	87.20	-
[151]	CNN	CT image	93.00	73.00	84.00	-
[161]	CNN	DICOM	-	91.50	-	-
[162]	Fine-Tuning DCNN	PD	-	-	99.10	-
[163]	Ensemble DL	CI	-	-	99.71	-
[164]	k-SVM	US	-	-	-	95.00
[165]	SVM RF	US	-	-	-	95.10
[166]	ANN SVM	US	-	96.00	-	-
[167]	RF	US	-	-	-	75.00
[168]	CNN	DICOM	82.40	85.00	83.00	-
[169]	ResNet18-based	PD	-	-	93.80	-
[170]	multiple-scale CNN	PD	-	-	82.20	-
[171]	Alexnet CNN	PD	-	-	86.00	-
[172]	CNN (BETNET)	US	-	98.30	-	-
[173]	ResNet	T	-	75.00	-	-
[174]	Xception	CT images	86.00	92.00	89.00	-
[175]	Google inception v3	HPI	-	-	95.00	-
[176]	CNN	T	81.80	86.10	85.10	-
[177]	CNN	T	78.00	85.00	82.10	-
[178]	CNN	T	80.60	80.10	80.30	-
[179]	CNN	US	-	-	77.00	-

Abbreviations: TIRADS (T), Cytological images (CI), Sono graphic images (SGI), Histo pathology images (HPI)

simulation, the percentage error is computed, yielding values of 5.337% for training, 7.407% for validation, and 5.092% for testing. The overall recognition rate stands at 94.4%, with an overall error rate of 5.6%. The receiver operating characteristic (ROC) curve is presented in

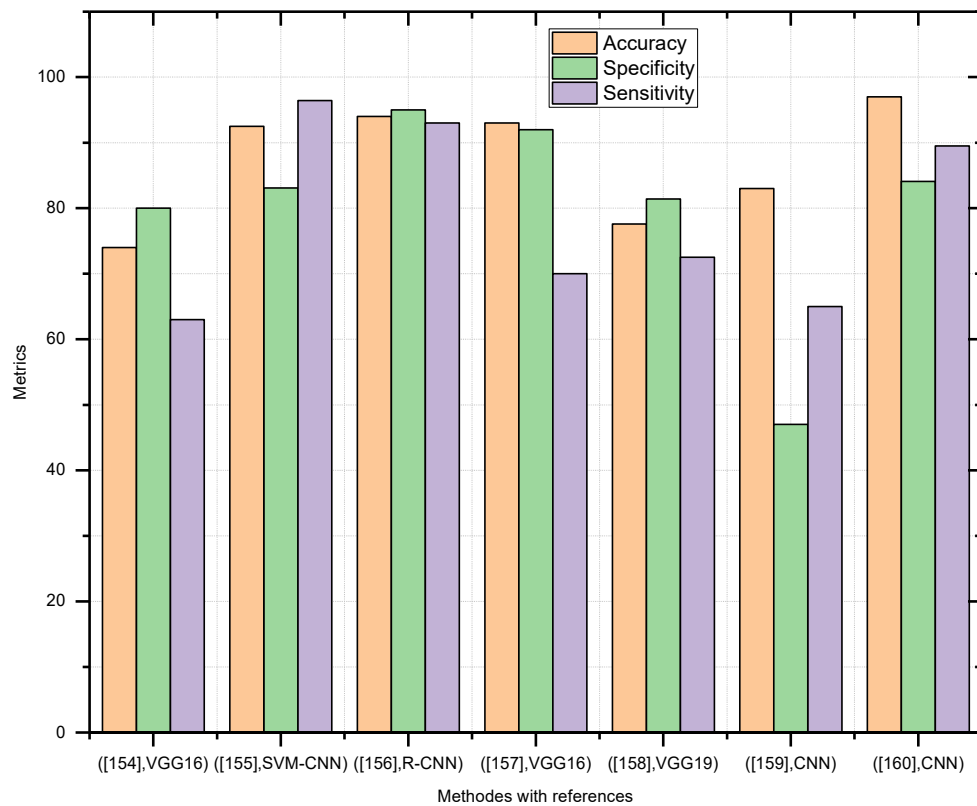


Figure 6. Performance assessment of TC frameworks in percentages (%) for US TCD [154], [155], [156–160].

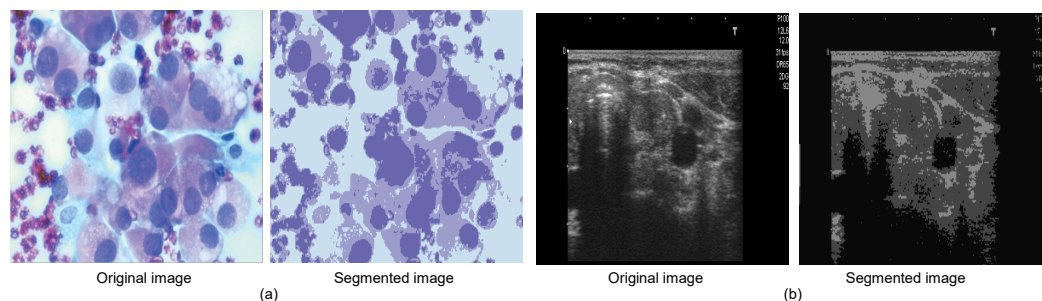


Figure 7. Thyroid segmentation example employing the K-Means method. (a) Imaging of medullary TC; (b) US imaging of the thyroid.

Figure 8. This example showcases the application of AI in TCD classification, achieving a high recognition rate with the provided dataset.

4. Advanced TCD using ViT and LLM

ViT and their advanced version, LLMs, have emerged as cutting-edge techniques in various AI-based biomedical tasks. Recently, researchers have begun applying these models to TCD. The following subsections provide a review of recent studies, along with a performance summary presented in Table 8.

4.1. ViT-based TCD methods

Vision Transformer (ViT) models are a type of DL model introduced in [155]. They have since become the foundation for many state-of-the-art natural language processing (NLP) and ML models. Transformers are designed to handle sequential data, making them suitable for various tasks beyond NLP as well [181–183]. Transformers in TCD

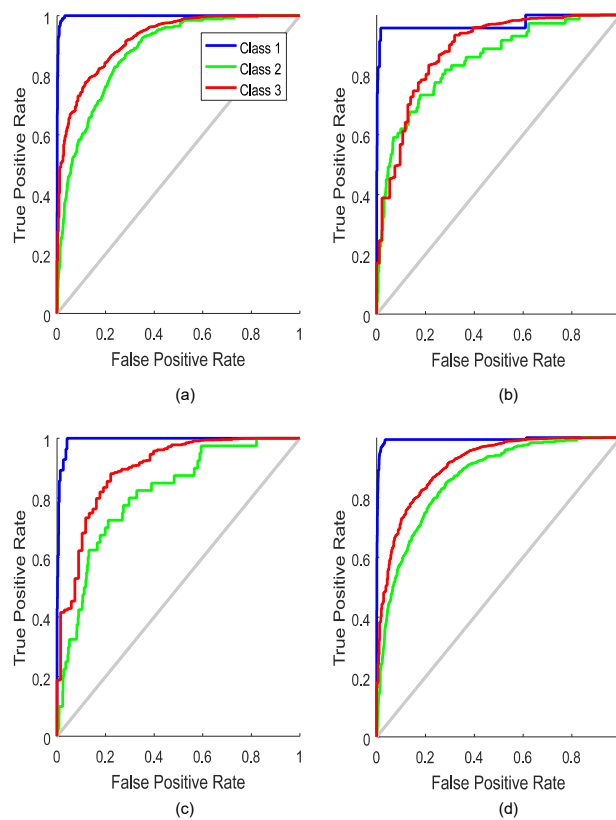


Figure 8. An example of TCD classification using ROC metric. (a) Training ROC; (b) Validation ROC; (c) Test ROC; (d) All ROC

enable efficient analysis of medical data, including literature and patient records, offering high accuracy. They uncover patterns, risk factors, and diagnostic clues, aiding early detection. This technology enhances diagnosis speed, fuels data-driven research, and promises improved patient care and oncology advancements [150,184]. Several studies have proposed the use of DL models, particularly Transformer-based models, for detecting TC from US images. For example, researchers in [185] developed a diagnostic system using DL (Deit, Swin Transformer, and Mixer-MLP) and metaheuristics to improve thyroid abnormality detection. The method in [185] ranked the models, leading to the selection of the best-performing models for ensemble learning. The optimization-based feature selection and random forest model achieved high accuracy on US and histopathological datasets, surpassing existing methods. This innovative approach eases the burden on healthcare professionals by enhancing TC diagnosis. The study [186], addressed the challenge of extracting important TN characteristics from clinical narratives in US reports using NLP. A team of experts developed annotation guidelines and tested five Transformer-based NLP models. Their GatorTron model, trained on a substantial text corpus, outperformed others, achieving the best F1-scores for extracting 16 TN characteristics and linking them to nodules. This pioneering work enables improved documentation quality of thyroid US reports and enhances patient outcomes assessment through electronic health records analysis. In [187], the study introduces a novel boundary-preserving assembly transformer UNet (BPAT-UNet) for precise US TN segmentation. This network incorporates a boundary point supervision module (BPSM) for boundary refinement and an adaptive multi-scale feature fusion module (AMFFM) for handling various scales of features. Additionally, an assembled Transformer module (ATM) improves boundary constraints and small object detection. Results demonstrated significantly improved segmentation accuracy compared to classical networks, achieving Dice similarity coefficients of 85.63% and 81.64% and HD95 values of 14.53 and 14.06 on private and public datasets, respectively. Chen et al.

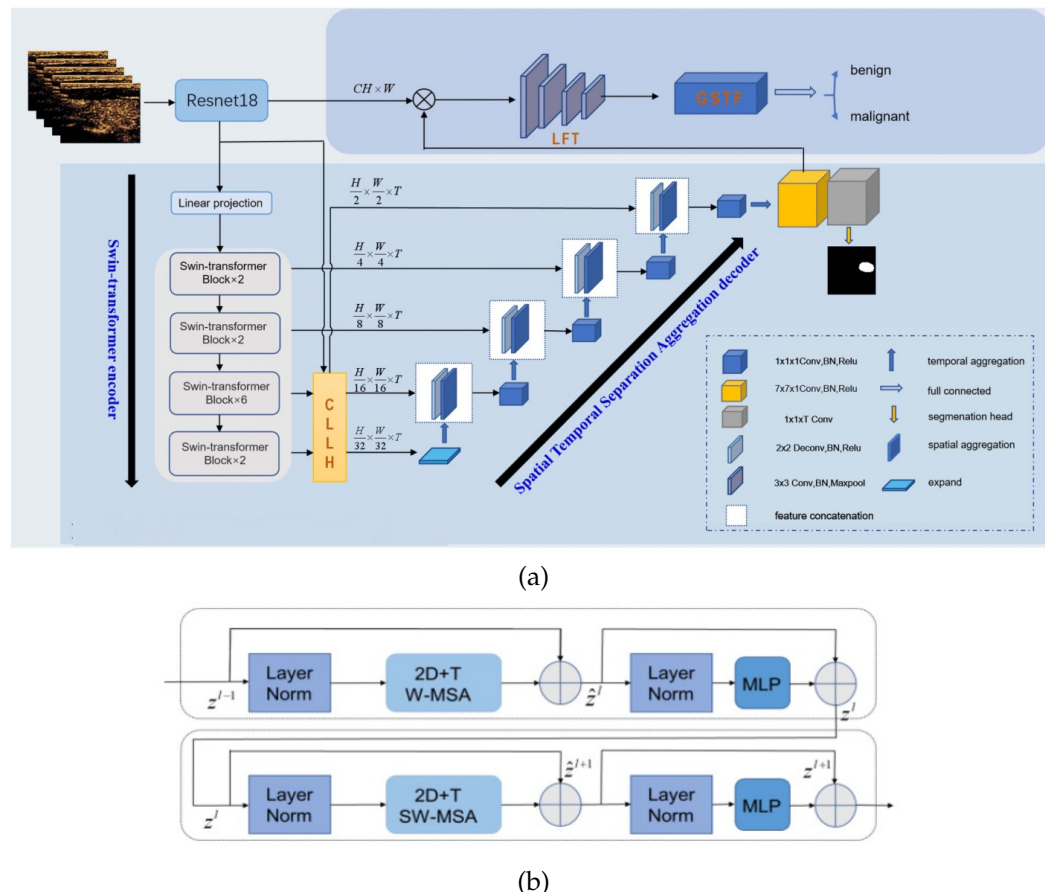


Figure 9. (a) The general framework of the suggested HEAT-Net, (b) Details of the Swin-Transformer block [188]

[188], introduce Trans-CEUS, a spatial-temporal Transformer-based model for real-time microvascular perfusion analysis using CEUS as it shown in Figure 9. It combines dynamic Swin-Transformer and collaborative learning to accurately segment lesions with unclear boundaries, achieving a Dice similarity coefficient of 82.41%. The model also attains a high diagnostic accuracy of 86.59% for distinguishing malignant and benign TN. This pioneering research highlights the effectiveness of Transformers in CEUS analysis and offers promising outcomes for TN segmentation and diagnosis from dynamic CEUS datasets.

DL has been instrumental in medical image segmentation, particularly for thyroid glands in US images. However, existing models face issues like the loss of low-level boundary features and limitations in capturing contextual features. In response, a hybrid Transformer UNet is introduced in [184]. It combines a 2D Transformer UNet with a multi-scale cross-attention Transformer and a 3D Transformer UNet with self-attention to improve representation and contextual information. The end-to-end network was evaluated on thyroid segmentation datasets, outperforming other methods in benchmark tests. The method shows promise for thyroid gland segmentation in US sequences. Dataset classification involves predicting a single label from sets with multiple instances, like pathology slides or medical text data. State-of-the-art methods often use complex attention architectures to model set interactions. However, when labeled sets are limited, as in medical applications, these architectures are challenging to train. To tackle this issue, a kernel-based framework is introduced in [189], connecting affinity kernels and attention architectures. This leads to simplified "affinitention" nets, which are applied to tasks like Set-Cifar10 classification, thyroid malignancy prediction, and patient text triage. Affinitention nets deliver competitive results, outperforming heuristic attention architectures and other methods. Jerbi

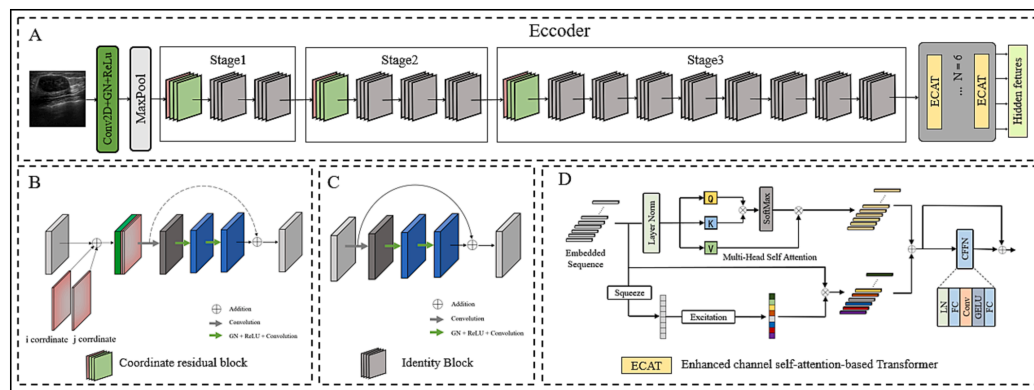


Figure 10. An example of the basic structure of encoder HEAT-Net for TC segmentation [191].

et al. in 2023 [190], incorporating CNNs and ViT, was employed to classify thyroid US images as either malignant or benign. A deep convolutional GAN was used to address data scarcity and imbalance. Various models, including VGG16, EfficientNetB0, ResNet50, ViT-B16, and hybrid ViT, were trained with both softmax and SVM classifiers. The hybrid ViT model, with SVM classification, outperformed others, achieving a 97.63% accuracy, showing promise for aiding doctors in diagnosing thyroid patients more effectively.

In [191], the authors introduce a novel U-shape segmentation model (Figure 10) combining CNN and Transformer structures to integrate local and long-range information. It uses coordinate residual blocks (CdRB) to encode position data, channel-enhanced self-attention-based Transformers for global feature enhancement, and a dual attention module for feature correlation and edge accuracy. The method outperforms state-of-the-art methods across various datasets, demonstrating adaptability and robustness in US image segmentation, potentially serving as a general segmentation tool. The work [192] addresses the challenge of accurately diagnosing malignant TN through US imaging. Existing CAD methods often struggle to maintain precise shape information and capture long-range dependencies. The proposed Transformer fusing CNN Network utilizes a large kernel module in a CNN branch for shape feature extraction and an enhanced Transformer module in another branch for remote pixel connections. A Multiscale fusion module integrates feature maps from both branches. Comparisons with other methods demonstrate the superiority of the proposed scheme and its effectiveness in nodule segmentation. Hypoparathyroidism is a major concern post-TC surgery, affecting patients' quality of life. Identifying and locating parathyroid glands via US images before surgery can help protect them. In [193] a dual-branch contextual-aware network with Transformer is proposed to reduce hypoparathyroidism incidence. It combines a Transformer for global context extraction and a feature encoder branch for local feature aggregation. A channel and spatial fusion module integrates information from both branches. The proposed method effectively addresses detail loss, establishing global and local feature dependencies. Experiments with an US image dataset demonstrate superior performance compared to existing methods. The thyroid gland plays a crucial role in regulating the human body's functions, making the identification of TN from US images important for medical diagnosis. However, the automatic segmentation of these nodules is challenging due to their heterogeneous appearance and background similarities. This framework [50] presents a novel framework AMSeg based on Swin-Unet architecture presented in Figure 11, which employs multi-scale anatomical features and late-stage fusion through adversarial training to address these challenges. Experimental results demonstrate the superiority of AMSeg in TN segmentation, achieving high dice, Hd95, Jaccard, and precision values. This end-to-end network offers promise for clinical applications, potentially replacing manual segmentation methods.

In [194], the authors harnessed NLP with a bidirectional encoder representations from Transformer (BERT) classifier to analyze unstructured clinical text data pertaining to recurrent papillary TC diagnosis. The BERT model achieved exceptional performance,

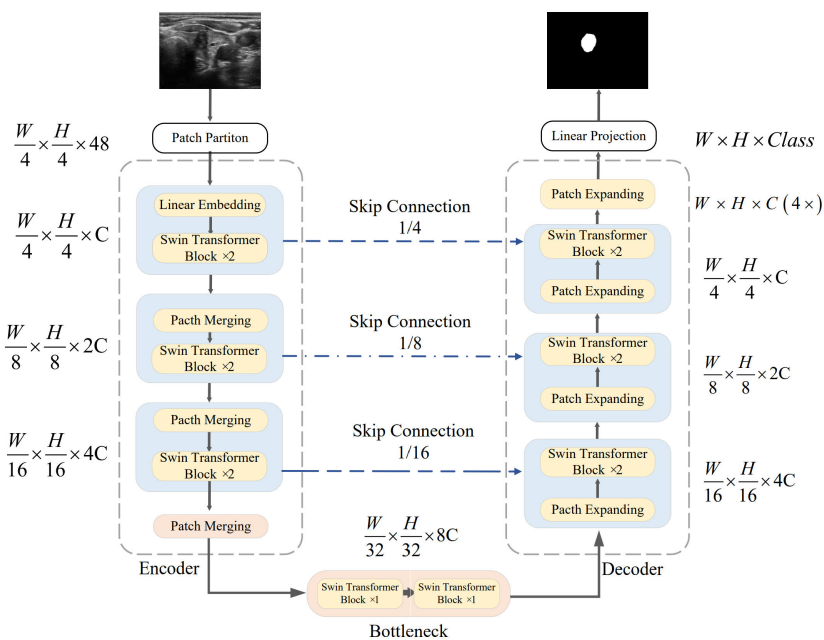


Figure 11. The Swin-UNet architecture [50].

boasting a 98.8% accuracy in binary recurrence classification. This approach streamlines the handling of unstructured patient information, eliminating the need for labour-intensive data refinement, and holds significant promise for training AI models in healthcare. The variability in features between benign and malignant TN, particularly in TIRADS level 3, can lead to inconsistent diagnoses and unnecessary biopsies. To address this in [195], ViT-based TCD, utilizes contrast learning to enhance diagnostic accuracy and biopsy specificity. By incorporating global and local features, this model minimizes the distinction between nodules of the same category. Test results indicate an accuracy of 86.9%, outperforming classical DL models. It offers automatic classification of TIRADS 3 and malignant nodules in US images, promising improved CAD and precise analysis. Optical coherence tomography (OCT) can aid in distinguishing normal and diseased thyroid tissue during surgery, but interpreting this type of image is challenging. Similarly, [196] explored various DL models for classifying thyroid diseases using 2D and 3D OCT data from 22 surgical patients with thyroid pathologies. The 3D ViTs model achieved the best performance, with an accuracy of 0.90 for normal versus abnormal classification. Custom models also excelled on open-access datasets. These findings suggest that combining OCT with DL can enable real-time, automatic identification of diseased tissue during thyroid surgery.

Accurate segmentation of TNs in US images is crucial for early TC diagnosis. Addressing the challenges posed by weak image edges and complex thyroid tissue structure, the study [197] introduces the LCA-Net method. It combines local features from CNNs and global context from Transformers, improving edge information capture. The model incorporates specific modules to handle different nodule sizes and positions, enhancing generalization. LCA-Net outperforms existing models on public datasets, demonstrating its potential for precise TN diagnosis in clinical settings. In this study [198], the authors focus on improving the prediction of lymph node metastasis in papillary thyroid carcinoma by combining whole slide histopathological images (WSIs) and clinical data. They introduce a Transformer-guided multi-modal multi-instance learning framework that effectively groups high-dimensional WSIs into low-dimensional feature embeddings and explores shared and specific features between modalities. The approach achieved an impressive area under curve (AUC) of 97.34% on their dataset, outperforming state-of-the-art methods by 1.27%, highlighting its potential in improving precision medicine decisions based on multi-modal medical data fusion. Diagnosing lymph node metastasis in papillary thyroid carcinoma typically relies on analyzing large WSIs. To enhance accuracy, a novel Transformer-guided

framework is introduced in [199], leveraging Transformers in three critical aspects. It incorporates a lightweight feature extractor, a clustering-based instance selection scheme, and a Transformer-MIL module for effective feature aggregation. The model further benefits from an attention-based mutual knowledge distillation paradigm. Experimental results on a WSI dataset outperform state-of-the-art methods by a significant margin, achieving a 2.72% higher AUC. Xiao et al. in [200] aims to address the challenges of diagnosing TC, particularly in cases where US images suffer from noise and artefacts, leading to a certain misdiagnosis rate in clinical practice. They highlight the need for further diagnosis using plain and contrast-enhanced CT scans. While plain CT provides valuable information, contrast-enhanced CT offers better contrast and can reflect organ margin erosion, a crucial symptom for TC diagnosis. However, the latter relies on the use of a contrast agent and exposes the patient to ionizing radiation. To mitigate these challenges, the authors propose an improved Unet architecture. Their approach involves using a convolutional Transformer module to learn global information from high-dimensional features. They also incorporate a texture feature module to extract local texture information from plain CT scans and integrate edge information obtained from superpixels as prior knowledge. The ultimate goal is to generate enhanced CT images with clear texture and higher quality, providing a valuable tool for TC diagnosis without the need for contrast agents and ionizing radiation. Histopathological images carry valuable information for tumour classification and disease prediction, but their size hinders direct use in CNNs. This study [201] introduces Pyramid Tokens-to-Token ViT, a lightweight architecture with multiple instance learning based on the ViTs. The method uses the Tokenization technique for feature extraction to reduce model parameters. It also incorporates an image pyramid to capture local and global features, significantly reducing computation. Experiments on thyroid pathology images yield superior results compared to CNN-based methods, balancing accuracy and efficiency. The authors in [202] aim to utilize multi-instance learning for the diagnosis of TC based on cytological smears. These smears lack multidimensional histological features, necessitating the mining of contextual information and diverse features for improved classification performance. To address these challenges, they introduce a novel algorithm called PyMLViT, which consists of two core modules. First, the pyramid token extraction module is designed to capture potential contextual information from smears. This module extracts multi-scale local features using a pyramid token structure and obtains global information through a ViTs structure with a self-attention mechanism. Second, they construct a multi-loss fusion module based on the conventional multi-instance learning framework. To enhance the diversity of supervised information, they carefully allocate bag and patch weights and incorporate slide-level annotations as pseudo-labels for patches during training. In Table 8, Transformer-based models' performance (in %) for TC diagnosis is summarized.

4.2. *LLM-based TCD methods*

The LLMs are advanced NLP model, trained on vast datasets to process, understand, and generate human-like text. Using DL and Transformer architectures, LLMs excel in tasks like answering questions, summarizing, translating, and creating content. In TCD, LLMs could be fine-tuned to assist in analyzing patient data, diagnostic reports, and medical literature, identifying patterns, and offering insights for early detection and personalized treatment. Their ability to process complex medical information enhances diagnostic accuracy, supports clinicians, and improves patient outcomes, making them invaluable in advancing thyroid cancer care and treatment. Several studies have suggested using LLM models for identifying thyroid cancer from US images. For instance, researchers in [203] evaluate a privacy-preserving LLM for extracting critical clinical information from thyroid cancer pathology reports. Using FastChat-T5, the model answered 1,008 questions about staging and recurrence risk across 84 reports. Concordance rates between the LLM and human reviewers averaged 89%, with the LLM completing tasks significantly faster (19.6 minutes vs. 206.9 minutes). While accurate for binary questions, challenges arose in complex queries. The findings highlight the potential of tailored LLMs for effi-

Table 8. Summary of Transformer and LLM-based models' performance (in %) for TC diagnosis.

Ref.	Transformer	Task	ACC	SEN	SPE	AUC	F1-score	Improvement
[185]	Swing BERT, RoBERTa, LongFormer, DeBERTa, and GatorTron	C	99.13	–	–	99.13	98.82	The diagnosis accuracy and the extract features of thyroid abnormality detection has been improved. The redundant features has reduced to avoid the overfitting.
[186]		C	97.10	98.80	92.80	–	96.50	The proposed model can achieve satisfactory classification accuracy and identify a large number of characteristics comparable to experienced radiologists and can save time and effort as well as deliver potential clinical application value
[188]	Trans-CEUS	S	86.59	–	–	–	–	Demonstrated significant improvement when compared to previous approaches, showcasing its effectiveness in the tasks of lesion segmentation and TN diagnosis.
[189]	Network	C	–	–	–	91.3	–	Attention nets outperform complex attention-based architectures and other competing methods in tasks such as thyroid malignancy prediction.
[190]	ViTs	C	97.63	–	–	–	96.67	The SVM classification produces better performance than the Softmax classification for all of the models with the Hybrid ViT
[194]	BERT	C	–	–	–	–	88.00	Analyze unstructured clinical text information on the diagnosis of the recurrent PTC efficiently.
[195]	ViT	C	86.90	87.10	86.10	–	92.4	Improve accuracy of diagnosis and specificity of biopsy recommendations. Minimize the representation distance between nodules of the same category
[196]	3Dvision	C	90.00	–	–	–	–	Efficiently classifying thyroid diseases
[198]	GMMML	P	93.88	–	–	97.34	94.65	Experimental results on the collected lymph node metastasis dataset demonstrate the efficiency of the proposed method
[199]	Tiny-ViT	P	–	–	–	98.35	92.97	Improve predict lymph node metastasis from WSIs efficiently using a novel Transformer-guided.
[201]	T2T-ViT	C	86.60	–	–	–	–	The model parameters are reduced, and the model performance and computation are greatly improved compared with CNN.
[202]	PyMLViT	C	87.50	–	–	–	–	Optimize the training process of the network.
[203]	FastChat-T5	MQA	88.86	–	–	–	–	Significant reduction in time for data extraction.
[204]	GPT-4	MQA	95.25	–	–	–	–	GPT-4 responses scored highest for accuracy, quality, and empathy compared to GPT-3.5 and doctors.
[205]	GPT-4	D	90.00	–	–	–	–	The diagnosis closely resembles human reports.
[206]	ChatGPT-4	D	86.00	–	–	–	–	Optimal performance in US diagnosis of thyroid nodules.
[207]	GPT-4o	D	93.00	–	–	–	–	High accuracy in diagnosis and management of thyroid nodules.
[208]	LlaMA2-13B	D	87.50	86.20	88.30	90.90	85.00	Diagnosis accuracy surpassed standalone CAD models and human performance.
[209]	BertTCR	P	96.60	100	100	100	95.80	High performance in predicting thyroid cancer-related immune.

Abbreviations: segmentation (S); Classification (C); Prediction (P); Medical question answering (MQA); Diagnosis (D).

cient, privacy-compliant clinical data extraction. Moving on, Raghunathan et al. [204] evaluate LLMs, including ChatGPT-3.5 and GPT-4, in addressing thyroid disease patient queries compared to verified doctors. Using a 4-point Likert scale, the proposed LLMs outperformed physicians in accuracy, quality, and empathy. GPT-4 scored highest across metrics. The findings highlight LLMs' potential to enhance patient communication, reduce clinician workload, and mitigate burnout by providing accurate and empathetic answers to complex medical questions in thyroid care. Wu et al. [206] evaluated the feasibility of leveraging LLMs like ChatGPT 4.0 to enhance thyroid nodule diagnosis using standardized reporting (TI-RADS) and pathology as the reference standard. Among 1161 ultrasound images analyzed, ChatGPT 4.0 outperformed others in consistency and diagnostic accuracy, especially when combined with image-to-text strategies. It matched or exceeded human-LLM interactions and showed potential to improve diagnostic efficiency while maintaining interpretability. Differently, Shah et al. [207] presented EndoGPT, a LLM-based tool developed for thyroid nodule management using GPT-4o, prompt engineering, and knowledge retrieval. Tested on 50 patient scenarios, it achieved a high overall concordance with expert surgeon plans, excelling in diagnosis and operational decisions, though less so in operation type (69%). While not a replacement for clinicians, EndoGPT highlights the potential of LLMs in aiding medical decision-making, education, and enhancing accessibility to clinical guidelines. Similarly, [208] introduced AIGC-CAD model for thyroid nodules. Inspired by ChatGPT, it integrates human-computer interaction to enhance diagnostic accuracy using 19,165 ultrasound cases. By combining DL models and semantic understanding, the model provides transparent diagnostic rationales and improves physician confidence. The model enhances junior radiologists' sensitivity and specificity by over 20%, bridging skill gaps. Its explainable and interactive features mark a paradigm shift in CAD applications. Wang et al. [205] evaluates GPT-4's capabilities in thyroid ultrasound diagnosis and treatment recommendations using 109 cases. GPT-4 excelled in report structuring, clarity, and professional terminology but showed limitations in diagnostic accuracy. The chain of thought method enhanced interpretability, and the AI-generated reports were largely

indistinguishable from human-written ones in a Turing Test. Zhang et al. [209] presented BertTCR, an advanced DL framework for predicting cancer-related immune status via T cell receptor (TCR) repertoire analysis. BertTCR leverages a pre-trained protein-BERT model to extract high-dimensional features, incorporating CNN, multiple instance learning, and ensemble techniques to enhance accuracy. Validated on datasets for thyroid and lung cancer, it achieves notable AUC improvements over existing methods. The framework's flexibility supports universal cancer detection and immune status assessment. BertTCR's findings emphasize its potential for early cancer detection, personalized medicine, and broad applications in immune-related diagnostics. Table 8 presents a summary of the performance of various LLM-based TCD methods across different metrics.

5. Limitations and challenges

Recognizing the obstacles in integrating AI solutions into healthcare practices, including infrastructural, regulatory, and cultural challenges, is essential. Highlighting the critical role of cross-disciplinary cooperation in seamlessly integrating AI into healthcare systems, thereby maximizing its beneficial impacts on patient health outcomes.

Although AI methodologies have shown promise in TC diagnosis, they face challenges that hinder the development of efficient solutions, lead to increased expenses, and limit their broad application. For precise detection of TC, it's essential to collect and securely consolidate all relevant data in a single repository, unless adopting federated learning (FL) approaches, as Himeur et al. suggest [210]. Following this, algorithms capable of identifying all forms of TC must be developed. Comprehensive TCD should include an extensive array of training and testing images, diagrams of nodules, and detailed classifications of nodule characteristics across different sizes, as Shah et al. recommend [211]. It's crucial for these datasets to be continually updated with data from MRI, CT scans, X-rays, and other clinical images to assess TC accurately. The inclusion of demographic details such as race, ethnicity, gender, and age is also necessary. Establishing a centralized database accessible to all healthcare facilities for testing, validating, and implementing AI algorithms on the collected data is critical, following Salazar et al.'s guidance [212]. Additionally, a succinct overview of further limitations and challenges yet to be addressed is provided.

(a) Clean and sufficient labelled data to ensure accuracy: In TC diagnosis, a major challenge is the lack of detailed, well-annotated datasets that thoroughly document the disease's incidence and progression. Elmore et al. [213] highlight the difficulty in collecting and validating TC-related data due to the absence of comprehensive clinical databases. AI algorithms struggle with accurate TC diagnosis because of limited labelled cases correlating with clinical outcomes, as noted by Park et al. [214]. Although large datasets are crucial for neural networks to produce accurate results, selective data incorporation during training is necessary to avoid harmful noise. Imaging modalities like CT and MRI, though available, are costly and not always accessible, as Ha et al. [31] point out. US imaging, combined with physical exams, fine-needle aspiration biopsies, or radioisotope scans, is preferred for its cost-effectiveness and accessibility. However, Zhu et al. [215] note that US accuracy in distinguishing malignant from benign nodules can vary and images may be noisy. Cancerous cells in thyroid tissue are often a small fraction of the total dataset, leading to a skewed distribution that can impair AI detection performance, as observed by Yao et al. [216]. Researchers face challenges in developing algorithms to handle limited, noisy, sparsely annotated, incomplete, or high-dimensional samples efficiently. Annotation is crucial but time-consuming and costly, impacting AI algorithm precision due to inconsistent labelling, as discussed by Sayed et al. [217] and Yao et al. [216].

(b) Hyperparameters of DL models: Designing the effective DL algorithm is crucial for overcoming different challenges, especially in diagnosing TC. The task of precisely differentiating between malignant and benign tumours, is complex due to their significant similarities, as highlighted in the study by Wang et al. [218]. Addressing this challenge may require significantly increasing the number of DL layers for feature extraction. However, such an increase can lead to longer processing times, particularly with large datasets, which

may delay timely cancer diagnoses for patients, as pointed out in the research by Lin et al. [30].

(c) Computation cost and storage limitations: Pose notable hurdles in algorithm development. Time complexity, a key measure in algorithm evaluation, assesses computational complexity by approximating the count of basic operations performed and its relationship with the size of input data. Typically represented as $O(n)$, where n is the size of the input, often measured by the bits required for its representation, this concept is thoroughly examined in the study by Al et al. [219]. Particularly in AI research related to TCD, researchers are tasked with finding algorithms that offer a harmonious blend of accuracy and computational efficiency. Their goal is to develop algorithms that can quickly process large datasets while maintaining precise results. Furthermore, the extensive amount of data used in these algorithms sometimes exceeds the storage capabilities, an issue underscored in the research by Lin et al. [30].

(d) Data loss and Error vulnerabilities: The shift towards digital medical records is crucial, notably in cancer diagnosis using slide images. This latter facilitates the use of AI for pathologic examinations [220]. Nonetheless, medical digitalization encounters specific challenges. There exists the danger of losing critical information during the digital conversion process and potential inaccuracies due to data compression methods applied in autoencoder algorithms. Thus, selecting the right digitalization technology is essential to ensure the preservation of data fidelity and authenticity [221]. The subtle contrast between the thyroid gland and surrounding tissues complicates accurate analysis and diagnosis of TC. Despite AI's inherent autonomy, it is prone to making errors. For example, training an algorithm with TCDs for identifying cancerous regions can lead to biased predictions if the training datasets are biased. These biases may then lead to a series of erroneous results, which could go unnoticed for a significant duration. Identifying and correcting the source of these errors, once recognized, can be a laborious process, as explored in the research by Karsa et al. [222].

(e) Unexplainable AI: The application of AI in healthcare sometimes results in "black box" outcomes, where the decision-making process lacks transparency and sufficient justification. This lack of clarity can make healthcare practitioners question the dependability of the results, possibly leading to incorrect choices and treatments for patients with TC. In essence, AI systems can operate as black boxes, providing outcomes without explicit and comprehensible rationales, a concern highlighted in the research by Sardianos et al. [223].

(f) Lack of cancer detection platform: A significant barrier in detecting various cancers, including TC, is the absence of platforms that facilitate the replication and evaluation of previous research. This gap presents a considerable challenge that hampers the assessment of AI algorithms' performance, thereby hindering improvements [132]. The presence of online platforms that offer cutting-edge algorithms, extensive datasets, and expert insights is crucial for assisting healthcare practitioners, specialists, researchers, and developers in making the right decisions with reduced chances of error. Moreover, this kind of platforms are vital in augmenting clinical diagnoses, as they enable more thorough Examination and assessment [224].

6. Future research directions

This segment delves into the anticipated developments of AI in identifying TC, scrutinizing forthcoming trends and advancements alongside their ethical repercussions. Ethical concerns encompass more than the immediate area of focus; issues regarding data privacy, responsibility, and fairness are also discussed. This part underscores research avenues poised to significantly improve TCD classification and prediction.

(a) Employing XAI: Integrating AI into decision-making is crucial but faces challenges due to its complexity and lack of clarity. To mitigate these issues, explainable artificial intelligence (XAI) seeks to make AI models more transparent, more accurate and confident decisions. This is particularly vital in healthcare, where understanding the rationale behind AI-generated outcomes is paramount. XAI has been applied to TCD, as evidenced in

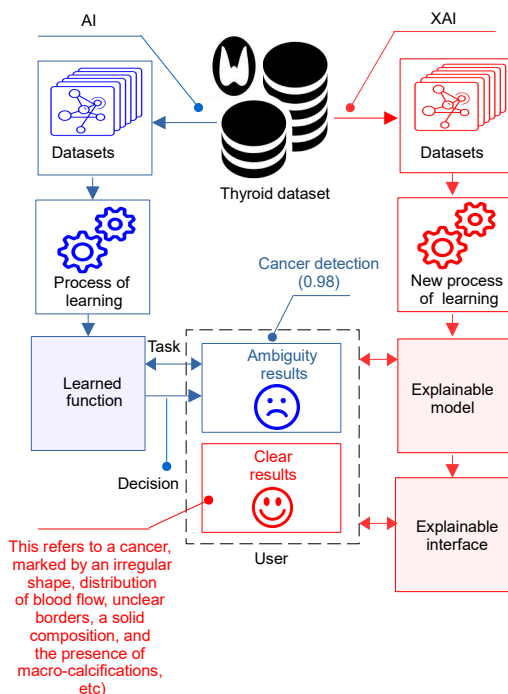


Figure 12. Diagram of XAI blocks for TCD.

studies by Lamy et al. [225], and Poceviciute et al. [226]. The differentiation between standard AI and XAI is showcased in Figure 12. Wildman et al. [144] proposed an XAI approach for detecting TC, enhancing the confidence of healthcare practitioners in AI predictions. XAI models clarify their reasoning, addressing the limitations associated with opaque "black box" algorithms.

(b) Using cloud, fog, and edge computing: The concept of edge networks merges edge computing with AI, allowing AI algorithms to operate closer to where data originates, a discussion brought forward by Sayed et al. [227]. This method enhances efficiency and cost-effectiveness for data-intensive applications, minimizing the requirement for extensive communication between patients and healthcare providers. By positioning data and storage closer to users in the healthcare field, this approach enables direct and swift access, a point highlighted by Alsalemi et al. [228]. To further improve the detection of TC within edge networks, fog computing is integrated. Fog computing introduces a distributed framework that bridges cloud computing and data generation sources, offering a versatile distribution of computational and storage capacities at key locations to boost overall system performance [229]. Cloud computing acts as a pivotal facilitator for the efficient functioning of AI-driven TCD systems, offering readily available access to data storage, servers, databases, networks, and applications for healthcare professionals, contingent upon internet connectivity. This integrated approach has proven its worth in medical scenarios, such as in the TC detection, as corroborated by several researches [230,231].

(c) Deep reinforcement learning (DRL): Reinforcement learning (RL), a branch of ML [232], enables agents to navigate and make decisions in evolving environments by engaging in a learning cycle of trial and error, observation, and interaction. The interest in leveraging RL for diagnosing untreatable diseases and enhancing the support for medical decision-making processes has grown recently. For example, Balaprakash et al. [233] apply RL in cancer data classification, whereas Li et al. [234] explore the use of deep RL for lymph node dataset segmentation. In this approach, pseudo-ground truths are created using RECIST-slices, facilitating the simultaneous tuning of lymph node bounding boxes through the collaborative efforts of a segmentation network and a policy network.

(d) Deep transfer learning (DTL): DTL is recognized as an effective approach to reduce overfitting and improve the precision of diagnostic tools [110,235]. This technique applies

the knowledge acquired from one domain to solve related issues in another, such as shortening the duration of training and minimizing the amount of data needed [217,236]. It is particularly useful in diagnosing TG. For example, the Enhance-Net model, described in [237], could act as a foundational model to boost the efficacy of a targeted DL model aimed at analyzing medical images in real-time. Furthermore, in [131], the research focuses on identifying pertinent characteristics of benign and malignant nodules using CNNs. By transferring insights from generic data to a dataset of US images, they achieve a fusion of hybrid semantic deep features. The application of transfer learning has also proven beneficial in categorizing images of TNs, as shown in [137].

(i) Federated learning (FL): FL has gained traction in healthcare applications due to its capacity to enhance patient data privacy across different healthcare settings [210]. The influence of environmental factors on human health, which can subsequently impact economic stability, is substantial. An increase in the incidence of thyroid gland disorders has been observed across diverse populations. ML plays a crucial role in addressing such health issues by leveraging collected data to train models capable of foreseeing severe health conditions. Considering the critical need for maintaining the confidentiality of patient information among various health institutions, FL stands out as an optimal framework for these purposes. Lee et al. [238] conducted a study comparing the effectiveness of FL with five traditional DL techniques in analyzing and detecting TC.

(e) Panoptic segmentation (PS): Accurately identifying and segmenting objects with varied and intersecting features continues to be a significant hurdle, especially in the medical field. To tackle this issue, several scholars have developed holistic and unified segmentation methods [239]. Panoptic segmentation has received considerable attention, merging the principles of instance and semantic segmentation to detect and delineate objects efficiently. Semantic segmentation involves the classification of each pixel into distinct categories, whereas instance segmentation focuses on delineating individual object instances. AI has been applied to this framework through either supervised or unsupervised instance segmentation learning techniques, making it highly applicable to medical scenarios [240].

(f) IoMIT and 3D-TCD: The internet of medical imaging thing (IoMIT) has gained substantial interest in the healthcare industry in recent years. IoMIT seeks to advance the quality of healthcare services and minimize treatment expenses by facilitating the exchange of medical information between patients and healthcare providers via interconnected devices equipped with wireless communication technology. An instance of such integration is showcased in [241], where an AI-enhanced solution for the preemptive identification of TC within the IoMIT paradigm is introduced. This method employs CNN to refine the distinction between benign and malignant nodules, aiming ultimately at life preservation. Additional investigations pertinent to IoMIT [242]. 2D US is a prevalent technique for evaluating TNs, yet its static imagery might not fully capture the nodules' complex structures. Consequently, there's a growing interest in utilizing three-dimensional (3D) US, which offers a holistic view of the lesion by reconstructing nodule characteristics, thereby facilitating enhanced discrimination between different diagnostic categories [243]. The capability of 3D US to analyze intricate growth patterns, edges, and forms from various perspectives and depths allows for a more accurate assessment of TNs' morphological features compared to 2D US.

(g) AI-based thyroid surgical techniques: As surgical practices face complex challenges, the essential role of AI-driven robotic assistance is becoming increasingly recognized. AI has the capability to navigate clinical intricacies by processing and leveraging large volumes of data, offering decision-making support with a precision that rivals that of medical experts [244]. Businesses are AI into surgical operations through the development of AI systems and the deployment of robots to aid surgeons in the operating room. These robots fulfil various functions, such as managing surgical tools, handling potentially contaminated materials and medical waste, conducting remote patient monitoring, and compiling patient information including electronic health records, vital signs, lab results, and video documentation [245]. It is therefore vital for surgeons to develop a comprehensive under-

standing of AI and its potential impacts on healthcare. While AI-enabled robotic surgery is still emerging, fostering interdisciplinary collaboration can accelerate the progress of AI technology, thereby improving surgical outcomes [246].

(h) Recommender systems (RSs): The vast amount of information produced by online medical platforms and electronic health records presents a challenge for TC patients seeking specific and accurate data [247]. Additionally, the substantial costs associated with healthcare data management can complicate the task of physicians handling a broad spectrum of patients and treatment alternatives. The implementation of RS has been suggested as a solution to improve decision-making within healthcare, reducing the load on both patients and oncologists [248,249]. Incorporating RS into digital health facilitates tailored recommendations, precise evaluation of large data sets, and stronger privacy measures, leveraging the capabilities of AI and ML technologies [250].

(k) Image and video compression, and denoising for TCD: The use of medical image and video compression plays a pivotal role in enhancing the detection and diagnosis of cancer, leveraging the advancements in digital imaging and telecommunications. This technological advancement allows for the efficient storage and transmission of high-resolution diagnostic images such as X-rays, MRIs, and CT scans, which are critical in identifying malignant tumors at early stages. Compression algorithms, both lossless and lossy, are meticulously designed to ensure that the integrity of the diagnostic information is maintained, making it possible for radiologists and oncologists to discern fine details crucial for accurate diagnosis. Furthermore, the reduced file sizes facilitate quicker transfer speeds across networks, enabling real-time collaboration and consultation among healthcare professionals worldwide, thereby significantly improving the speed and accuracy of cancer diagnosis. This is especially vital in remote or resource-limited settings where access to high-quality healthcare and specialist consultations might be restricted, thus democratizing the access to crucial diagnostic services and improving patient outcomes [251–255]. In addition, applying denoising techniques to medical images before training can substantially improve the accuracy of TCD classification and decision-making processes [256].

(l) Features selection: The information gain (IG) method is useful in simplifying the classification of medical images. Researchers are encouraged to explore its usefulness for detecting TC by identifying the most informative features that distinguish between malignant and benign TNs. The process begins with data collection, where a comprehensive dataset containing relevant features, such as patient demographics, ultrasound characteristics, biopsy results, genetic markers, and blood test results, is gathered. Each instance in the dataset is labelled as benign or malignant based on definitive diagnostic methods. In the preprocessing stage, the data is cleaned by handling missing values and outliers and normalizing if necessary. Feature engineering may also be performed to create new features that enhance predictive power. The IG for each feature is then calculated, measuring how much it contributes to the classification. Features with high IG are considered more informative and are used to build a predictive model for TC detection. This method helps in selecting the most relevant features, thereby improving the accuracy and efficiency of the diagnostic process.

(m) Generating synthetic datasets: To advance TCD, future research should focus on enhancing dataset quality and diversity. Developing well-annotated datasets remains a challenge, which can be addressed through innovative techniques such as synthetic data generation, data augmentation, and multi-modal integration. Future work could explore more effective synthetic data generation methods, including enhanced GANs and variational DAEs, to create diverse, high-quality datasets that improve diagnostic accuracy and represent rare cancer subtypes [257]. Further investigation into advanced data augmentation strategies, such as complex image transformations and domain adaptation, could enhance model generalization by expanding dataset variability [258]. Additionally, multi-modal integration, combining imaging, genomics, and clinical data, holds promise for improving robustness and predictive performance through deep learning models and novel fusion strategies.

(n) Employing SSL: self-supervised learning (SSL) offers a promising avenue for feature extraction in TCDs, particularly when working with large volumes of unannotated medical images. By leveraging unlabeled data, SSL techniques can learn meaningful and discriminative representations, reducing the dependency on extensive manual annotation efforts. This approach has shown the potential to improve the robustness and generalization of diagnostic models by capturing complex patterns within medical imaging data. Incorporating SSL strategies could further enhance the development of automated diagnostic tools, especially in data-limited scenarios. Therefore, a dedicated discussion of SSL methods, including their applications and potential benefits in the TCD field, has been added to provide a comprehensive overview of emerging advancements. Recent studies have highlighted the effectiveness of SSL in medical image classification. For instance, [259] discusses various SSL strategies and their applications in medical imaging, emphasizing their potential to improve diagnostic performance. Additionally, research published in [260] explores SSL pre-training approaches, such as contrastive and masked modelling, demonstrating their superiority over traditional supervised methods in medical imaging tasks.

7. Conclusion

This investigation delves deeply into ML and DL, highlighting their growing prominence due to their enhanced precision over other methods. It comprehensively reviews various algorithms and training models, discussing their benefits and drawbacks. Specifically, DL techniques are celebrated for their application in a myriad of real-world scenarios, notably for their generalization capabilities and resilience to noise. Nevertheless, significant challenges obstruct the full adoption of DL in detecting TC, with the lack of clean data and appropriate platforms being primary concerns. Tackling these data challenges with detailed precision is essential for creating effective and robust models for detecting more complex cancer stages.

Future research should aim at overcoming these hurdles and improving TCD classification and prediction methods. This study highlights the urgent need for increased research focus on TC diagnostics to match the high precision expectations of healthcare practitioners. While cancer detection in two or three dimensions is progressing, the limited expertise in handling various geometric transformations and multi-dimensional data compromises the accuracy of diagnosing life-threatening diseases. Therefore, it is vital to innovate in distinguishing between cancerous nodule sizes. Such innovations could significantly speed up treatment, improve diagnostic precision, foster proactive epidemiological tracking, and reduce death rates. Novel technologies like XAI, edge computing, DTL, RL, FL for privacy-preserving mechanisms, and remote sensing are paving new paths in AI-based TCD research. These developments are crucial for medical professionals, simplifying the diagnostic process, reducing detection times, and enhancing patient confidentiality. Future research will explore the impact of these advanced technologies further. The objective is to create a major transformation in cancer detection approaches by crafting advanced, privacy-focused technologies for the identification of TC and extending into domains like Telehealth.

Acronyms and Abbreviations

Data availability

Data will be made available on request.

Conflict of Interest

The authors declare no conflicts of interest.

References

1. Himeur, Y.; Al-Maadeed, S.; Varlamis, I.; Al-Maadeed, N.; Abualsaud, K.; Mohamed, A. Face mask detection in smart cities using deep and transfer learning: lessons learned from the COVID-19 pandemic. *Systems* **2023**, *11*, 107.
2. Chouchane, A.; Ouamane, A.; Himeur, Y.; Mansoor, W.; Atalla, S.; Benzaibak, A.; Boudellal, C. Improving CNN-based Person Re-identification using score Normalization. In Proceedings of the 2023 IEEE International Conference on Image Processing (ICIP). IEEE, 2023, pp. 2890–2894.
3. Himeur, Y.; Al-Maadeed, S.; Almaadeed, N.; Abualsaud, K.; Mohamed, A.; Khattab, T.; Elharrouss, O. Deep visual social distancing monitoring to combat COVID-19: A comprehensive survey. *Sustainable cities and society* **2022**, *85*, 104064.
4. Sohail, S.S.; Farhat, F.; Himeur, Y.; Nadeem, M.; Madsen, D.Ø.; Singh, Y.; Atalla, S.; Mansoor, W. Decoding ChatGPT: A Taxonomy of Existing Research, Current Challenges, and Possible Future Directions. *Journal of King Saud University-Computer and Information Sciences* **2023**, p. 101675.
5. Himeur, Y.; Elnour, M.; Fadli, F.; Meskin, N.; Petri, I.; Rezgui, Y.; Bensaali, F.; Amira, A. AI-big data analytics for building automation and management systems: a survey, actual challenges and future perspectives. *Artificial Intelligence Review* **2023**, *56*, 4929–5021.
6. Calisto, F.M.; Nunes, N.; Nascimento, J.C. Modeling adoption of intelligent agents in medical imaging. *International Journal of Human-Computer Studies* **2022**, *168*, 102922.
7. Amine Becha and, Y.E.; Medjoudj, R.; Himeur, Y.; Amira, A. Harnessing Transformers: A Leap Forward in Lung Cancer Image Detection. In Proceedings of the 2022 6th International Conference on Signal Processing and Information Security (ICSPIS). IEEE, 2023, pp. 1–6.
8. Habchi, Y.; Himeur, Y.; Kheddar, H.; Boukabou, A.; Atalla, S.; Chouchane, A.; Ouamane, A.; Mansoor, W. AI in Thyroid Cancer Diagnosis: Techniques, Trends, and Future Directions. *Systems* **2023**, *11*, 519.
9. Salem, H.S. Cancer status in the Occupied Palestinian Territories: types; incidence; mortality; sex, age, and geography distribution; and possible causes. *Journal of Cancer Research and Clinical Oncology* **2023**, *149*, 5139–5163.
10. Deng, Y.; Li, H.; Wang, M.; Li, N.; Tian, T.; Wu, Y.; Xu, P.; Yang, S.; Zhai, Z.; Zhou, L.; et al. Global burden of thyroid cancer from 1990 to 2017. *JAMA network open* **2020**, *3*, e208759–e208759.
11. Castellana, M.; Piccardo, A.; Virili, C.; Scappaticcio, L.; Grani, G.; Durante, C.; Giovanella, L.; Trimboli, P. Can ultrasound systems for risk stratification of thyroid nodules identify follicular carcinoma? *Cancer cytopathology* **2020**, *128*, 250–259.
12. Hitu, L.; Gabora, K.; Bonci, E.A.; Piciu, A.; Hitu, A.C.; Štefan, P.A.; Piciu, D. MicroRNA in Papillary Thyroid Carcinoma: A Systematic Review from 2018 to June 2020. *Cancers* **2020**, *12*, 3118.
13. Giovanella, L.; Treglia, G.; Iakovou, I.; Mihailovic, J.; Verburg, F.A.; Luster, M. EANM practice guideline for PET/CT imaging in medullary thyroid carcinoma. *European journal of nuclear medicine and molecular imaging* **2020**, *47*, 61–77.
14. Ferrari, S.M.; Elia, G.; Ragusa, F.; Ruffilli, I.; La Motta, C.; Paparo, S.R.; Patrizio, A.; Vita, R.; Benvenga, S.; Materazzi, G.; et al. Novel treatments for anaplastic thyroid carcinoma. *Gland surgery* **2020**, *9*, S28.
15. Khammari, M.; Chouchane, A.; Ouamane, A.; Bessaoudi, M.; Himeur, Y.; Hassaballah, M.; et al. High-order knowledge-based Discriminant features for kinship verification. *Pattern Recognition Letters* **2023**, *175*, 30–37.
16. Hamza, A.; Lekouaghet, B.; Himeur, Y. Hybrid Whale-Mud-Ring Optimization for Precise Color Skin Cancer Image Segmentation. In Proceedings of the 2022 6th International Conference on Signal Processing and Information Security (ICSPIS). IEEE, 2023, pp. 1–6.
17. Tessler, F.N.; Middleton, W.D.; Grant, E.G. Thyroid imaging reporting and data system (TI-RADS): a user's guide. *Radiology* **2018**, *287*, 29–36.
18. Zhou, H.; Jin, Y.; Dai, L.; Zhang, M.; Qiu, Y.; Tian, J.; Zheng, J.; et al. Differential diagnosis of benign and malignant thyroid nodules using deep learning radiomics of thyroid ultrasound images. *European Journal of Radiology* **2020**, *127*, 108992.
19. Nayak, R.; Nawar, N.; Webb, J.; Fatemi, M.; Alizad, A. Impact of imaging cross-section on visualization of thyroid microvessels using ultrasound: Pilot study. *Scientific reports* **2020**, *10*, 1–9.
20. Kumar, V.; Webb, J.; Gregory, A.; Meixner, D.D.; Knudsen, J.M.; Callstrom, M.; Fatemi, M.; Alizad, A. Automated segmentation of thyroid nodule, gland, and cystic components from ultrasound images using deep learning. *IEEE Access* **2020**, *8*, 63482–63496.

21. Hahn, S.Y.; Shin, J.H.; Oh, Y.L.; Park, K.W.; Lim, Y. comparison Between fine needle Aspiration and core needle Biopsy for the Diagnosis of thyroid Nodules: Effective Indications According to US Findings. *Scientific reports* **2020**, *10*, 1–7.
22. Ullah, H.; Saba, T.; Islam, N.; Abbas, N.; Rehman, A.; Mehmood, Z.; Anjum, A. An ensemble classification of exudates in color fundus images using an evolutionary algorithm based optimal features selection. *Microscopy research and technique* **2019**, *82*, 361–372.
23. Wang, X.; Zhang, J.; Yang, S.; Xiang, J.; Luo, F.; Wang, M.; Zhang, J.; Yang, W.; Huang, J.; Han, X. A generalizable and robust deep learning algorithm for mitosis detection in multicenter breast histopathological images. *Medical Image Analysis* **2023**, *84*, 102703.
24. Wang, Y.; Yue, W.; Li, X.; Liu, S.; Guo, L.; Xu, H.; Zhang, H.; Yang, G. Comparison study of radiomics and deep learning-based methods for thyroid nodules classification using ultrasound images. *Ieee Access* **2020**, *8*, 52010–52017.
25. Zhang, B.; Tian, J.; Pei, S.; Chen, Y.; He, X.; Dong, Y.; Zhang, L.; Mo, X.; Huang, W.; Cong, S.; et al. Machine learning-assisted system for thyroid nodule diagnosis. *Thyroid* **2019**, *29*, 858–867.
26. Yang, C.Q.; Gardiner, L.; Wang, H.; Hueman, M.T.; Chen, D. Creating prognostic systems for well-differentiated thyroid cancer using machine learning. *Frontiers in endocrinology* **2019**, *10*, 288.
27. Liu, Y.; Liang, J.; Peng, S.; Wang, W.; Xiao, H. A deep-learning model to assist thyroid nodule diagnosis and management—Authors' reply. *The Lancet Digital Health* **2021**, *3*, e411–e412.
28. Iesato, A.; Nucera, C. Role of regulatory non-coding RNAs in aggressive thyroid cancer: Prospective applications of neural network analysis. *Molecules* **2021**, *26*, 3022.
29. Sharifi, Y.; Bakhshali, M.A.; Dehghani, T.; DanaiAshgari, M.; Sargolzaei, M.; Eslami, S. Deep learning on ultrasound images of thyroid nodules. *Biocybernetics and Biomedical Engineering* **2021**, *41*, 636–655.
30. Lin, Y.J.; Chao, T.K.; Khalil, M.A.; Lee, Y.C.; Hong, D.Z.; Wu, J.J.; Wang, C.W. Deep learning fast screening approach on cytological whole slides for thyroid cancer diagnosis. *Cancers* **2021**, *13*, 3891.
31. Ha, E.J.; Baek, J.H. Applications of machine learning and deep learning to thyroid imaging: where do we stand? *Ultrasoundography* **2021**, *40*, 23.
32. Wu, X.L.; Li, M.; Cui, X.w.; Xu, G. Deep multimodal learning for lymph node metastasis prediction of primary thyroid cancer. *Physics in Medicine & Biology* **2022**.
33. Pavithra, S.; Yamuna, G.; Arunkumar, R. Deep Learning Method for Classifying Thyroid Nodules Using Ultrasound Images. In Proceedings of the 2022 International Conference on Smart Technologies and Systems for Next Generation Computing (ICSTSN). IEEE, 2022, pp. 1–6.
34. Paul, R.; Juliano, A.; Faquin, W.; Chan, A.W. An Artificial Intelligence Ultrasound Platform for Screening and Staging of Thyroid Cancer. *International Journal of Radiation Oncology, Biology, Physics* **2022**, *112*, e8.
35. Ilyas, M.; Malik, H.; Adnan, M.; Bashir, U.; Bukhari, W.A.; Khan, M.I.A.; Ahmad, A. Deep Learning based Classification of Thyroid Cancer using Different Medical Imaging Modalities: A Systematic Review **2022**.
36. Kheddar, H.; Hemis, M.; Himeur, Y.; Megías, D.; Amira, A. Deep Learning for Diverse Data Types Steganalysis: A Review. *arXiv preprint arXiv:2308.04522* **2023**.
37. Lasseck, M. Audio-based Bird Species Identification with Deep Convolutional Neural Networks. In Proceedings of the CLEF (Working Notes), 2018.
38. Zhou, W.; Wang, Z.; Xie, W. Weighted signal-to-noise ratio robust design for a new double sampling npx chart. *Computers & Industrial Engineering* **2020**, *139*, 106124.
39. The ThyroidOmics Consortium. Available online: <https://transfer.sysepi.medizin.uni-greifswald.de/thyroidomics/>. Accessed: 2021-03-01.
40. Thyroid Disease Data Set. Available online: <https://archive.ics.uci.edu/ml/datasets/thyroid+disease>. Accessed: 2021-03-01.
41. Knowledge Extraction based on Evolutionary Learning. Available online: <https://sci2s.ugr.es/keel/dataset.php?cod=67>. Accessed: 2021-03-01.
42. Gene Expression Omnibus. Available online: <https://www.ncbi.nlm.nih.gov/geo/>. Accessed: 2021-03-01.
43. The digital database of Thyroid Ultrasound Images. Available online: <http://cimalab.intec.co/?lang=en&mod=project&id=31>. Accessed: 2021-03-01.
44. The National Cancer Registration and Analysis Service. Available online: http://www.ncin.org.uk/about_ncin/. Accessed: 2021-03-01.

45. The Prostate, Lung, Colorectal and Ovarian (PLCO) Cancer Screening Trial . Available online: <https://prevention.cancer.gov/major-programs/prostate-lung-colorectal-and-ovarian-cancer-screening-trial>. Accessed: 2021-03-01.
46. Liu, C.; Huang, Y.; Ozolek, J.A.; Hanna, M.G.; Singh, R.; Rohde, G.K. SetSVM: an approach to set classification in nuclei-based cancer detection. *IEEE Journal of Biomedical and Health Informatics* **2018**, *23*, 351–361.
47. Zhang, S.; Du, H.; Jin, Z.; Zhu, Y.; Zhang, Y.; Xie, F.; Zhang, M.; Jiao, Z.; Tian, X.; Zhang, J.; et al. Integrating Clinical Knowledge in a Thyroid Nodule Classification Model Based on. In Proceedings of the 2019 IEEE International Ultrasonics Symposium (IUS). IEEE, 2019, pp. 2334–2336.
48. Zhang, H.; Zhao, C.; Guo, L.; Li, X.; Luo, Y.; Lu, J.; Xu, H. Diagnosis of Thyroid Nodules in Ultrasound Images Using Two Combined Classification Modules. In Proceedings of the 2019 12th International Congress on Image and Signal Processing, BioMedical Engineering and Informatics (CISP-BMEI). IEEE, 2019, pp. 1–5.
49. Chen, D.; Zhang, J.; Li, W. Thyroid Nodule Classification Using Two Levels Attention-Based Bi-Directional LSTM with Ultrasound Reports. In Proceedings of the 2018 9th International Conference on Information Technology in Medicine and Education (ITME). IEEE, 2018, pp. 309–312.
50. Ma, X.; Sun, B.; Liu, W.; Sui, D.; Chen, J.; Tian, Z. AMSeg: A Novel Adversarial Architecture based Multi-scale Fusion Framework for Thyroid Nodule Segmentation. *IEEE Access* **2023**.
51. Sajeev, V.; Vyshnavi, A.H.; Namboori, P.K. Thyroid Cancer Prediction Using Gene Expression Profile, Pharmacogenomic Variants And Quantum Image Processing In Deep Learning Platform-A Theranostic Approach. In Proceedings of the 2020 International Conference for Emerging Technology (INCET). IEEE, 2020, pp. 1–5.
52. Shankarlal, B.; Sathya, P. Performance Analysis of Thyroid Tumor Detection and Segmentation Using PCA-Based Random Classification Method. In *Innovations in Electrical and Electronics Engineering*; Springer, 2020; pp. 833–841.
53. Soulaymani, A.; Aschawa, H. Epidemiological Study of Thyroid Carcinoma Using Principal Component Analysis. *Journal of Clinical Epigenetics* **2018**, *4*, 9.
54. Cui, L.; Ge, L.; Gan, H.; Liu, X.; Zhang, Y. Ovarian Cancer Identification Based On Feature Weighting For High-throughput Mass Spectrometry Data. *Journal of Systems Biology* **2018**, *1*, 1.
55. Al-Batah, M.; Zaqaibeh, B.; Alomari, S.A.; Alzboon, M.S. Gene Microarray Cancer Classification using Correlation Based Feature Selection Algorithm and Rules Classifiers. *International Journal of Online & Biomedical Engineering* **2019**, *15*.
56. Jain, I.; Jain, V.K.; Jain, R. Correlation feature selection based improved-binary particle swarm optimization for gene selection and cancer classification. *Applied Soft Computing* **2018**, *62*, 203–215.
57. Rustam, Z.; Maghfirah, N. Correlated based SVM-RFE as feature selection for cancer classification using microarray databases. In Proceedings of the AIP Conference Proceedings. AIP Publishing LLC, 2018, Vol. 2023, p. 020235.
58. Bhalla, S.; Kaur, H.; Kaur, R.; Sharma, S.; Raghava, G.P. Expression based biomarkers and models to classify early and late-stage samples of Papillary Thyroid Carcinoma. *PLoS One* **2020**, *15*, e0231629.
59. O'Dea, D.; Bongiovanni, M.; Sykotis, G.P.; Ziros, P.G.; Meade, A.D.; Lyng, F.M.; Malkin, A. Raman spectroscopy for the preoperative diagnosis of thyroid cancer and its subtypes: An in vitro proof-of-concept study. *Cytopathology* **2019**, *30*, 51–60.
60. Sudarshan, V.K.; Mookiah, M.R.K.; Acharya, U.R.; Chandran, V.; Molinari, F.; Fujita, H.; Ng, K.H. Application of wavelet techniques for cancer diagnosis using ultrasound images: a review. *Computers in biology and medicine* **2016**, *69*, 97–111.
61. Haji, S.O.; Yousif, R.Z. A Novel Run-length based wavelet features for Screening Thyroid Nodule Malignancy. *Brazilian Archives of Biology and Technology* **2019**, *62*.
62. Yu, B.; Wang, Z.; Zhu, R.; Feng, X.; Qi, M.; Li, J.; Zhao, R.; Huang, L.; Xin, R.; Li, F.; et al. The transverse ultrasonogram of thyroid papillary carcinoma has a better prediction accuracy than the longitudinal one. *IEEE Access* **2019**, *7*, 100763–100770.
63. Nguyen, D.T.; Pham, T.D.; Batchuluun, G.; Yoon, H.S.; Park, K.R. Artificial intelligence-based thyroid nodule classification using information from spatial and frequency domains. *Journal of clinical medicine* **2019**, *8*, 1976.
64. Poudel, P.; Illanes, A.; Arens, C.; Hansen, C.; Friebe, M. Active contours extension and similarity indicators for improved 3D segmentation of thyroid ultrasound images. In Proceedings of

the Medical Imaging 2017: Imaging Informatics for Healthcare, Research, and Applications. International Society for Optics and Photonics, 2017, Vol. 10138, p. 1013803.

- 65. Poudel, P.; Hansen, C.; Sprung, J.; Friebe, M. 3D segmentation of thyroid ultrasound images using active contours. *Current Directions in Biomedical Engineering* **2016**, *2*, 467–470.
- 66. Nugroho, H.A.; Nugroho, A.; Choridah, L. Thyroid nodule segmentation using active contour bilateral filtering on ultrasound images. In Proceedings of the 2015 International Conference on Quality in Research (QiR). IEEE, 2015, pp. 43–46.
- 67. Xie, J.; Guo, L.; Zhao, C.; Li, X.; Luo, Y.; Jianwei, L. A Hybrid Deep Learning and Hand-crafted Features based Approach for Thyroid Nodule Classification in Ultrasound Images. In Proceedings of the Journal of Physics: Conference Series. IOP Publishing, 2020, Vol. 1693, p. 012160.
- 68. Mei, X.; Dong, X.; Deyer, T.; Zeng, J.; Trafalis, T.; Fang, Y. Thyroid nodule benignity prediction by deep feature extraction. In Proceedings of the 2017 IEEE 17th International Conference on Bioinformatics and Bioengineering (BIBE). IEEE, 2017, pp. 241–245.
- 69. Dinčić, M.; Todorović, J.; Ostočić, J.N.; Kovačević, S.; Dunderović, D.; Lopičić, S.; Spasić, S.; Radojević-Škodrić, S.; Stanislavljević, D.; Ilić, A.Ž. The fractal and GLCM textural parameters of chromatin may be potential biomarkers of papillary thyroid carcinoma in Hashimoto's thyroiditis specimens. *Microscopy and Microanalysis* **2020**, *26*, 717–730.
- 70. Kalaimani, I. Analysis for the Prediction of Thyroid Disease by Using ICA and Optimal Kernel SVM Approach. *International Journal of Emerging Technology and Innovative Engineering* **2019**, *5*.
- 71. Ahmad, W.; Huang, L.; Ahmad, A.; Shah, F.; Iqbal, A.; Saeed, A. Thyroid diseases forecasting using a hybrid decision support system based on ANFIS, k-NN and information gain method. *J Appl Environ Biol Sci* **2017**, *7*, 78–85.
- 72. Nugroho, H.A.; Nugroho, A.; Frannita, E.L.; Ardiyanto, I.; et al. Classification of thyroid ultrasound images based on shape features analysis. In Proceedings of the 2017 10th Biomedical Engineering International Conference (BMEiCON). IEEE, 2017, pp. 1–5.
- 73. Mourad, M.; Moubayed, S.; Dezube, A.; Mourad, Y.; Park, K.; Torreblanca-Zanca, A.; Torrecilla, J.S.; Cancilla, J.C.; Wang, J. Machine Learning and feature Selection Applied to SeeR Data to Reliably Assess thyroid cancer prognosis. *Scientific Reports* **2020**, *10*, 1–11.
- 74. Song, H.; Dong, C.; Zhang, X.; Wu, W.; Chen, C.; Ma, B.; Chen, F.; Chen, C.; Lv, X. Rapid identification of papillary thyroid carcinoma and papillary microcarcinoma based on serum Raman spectroscopy combined with machine learning models. *Photodiagnosis and Photodynamic Therapy* **2022**, *37*, 102647.
- 75. Acharya, U.R.; Faust, O.; Sree, S.V.; Molinari, F.; Suri, J.S. ThyroScreen system: high resolution ultrasound thyroid image characterization into benign and malignant classes using novel combination of texture and discrete wavelet transform. *Computer methods and programs in biomedicine* **2012**, *107*, 233–241.
- 76. Nugroho, H.A.; Frannita, E.L.; Ardiyanto, I.; Choridah, L.; et al. Computer aided diagnosis for thyroid cancer system based on internal and external characteristics. *Journal of King Saud University-Computer and Information Sciences* **2021**, *33*, 329–339.
- 77. Sun, C.; Zhang, Y.; Chang, Q.; Liu, T.; Zhang, S.; Wang, X.; Guo, Q.; Yao, J.; Sun, W.; Niu, L. Evaluation of a deep learning-based computer-aided diagnosis system for distinguishing benign from malignant thyroid nodules in ultrasound images. *Medical Physics* **2020**, *47*, 3952–3960.
- 78. Liu, C.; Chen, S.; Yang, Y.; Shao, D.; Peng, W.; Wang, Y.; Chen, Y.; Wang, Y. The value of the computer-aided diagnosis system for thyroid lesions based on computed tomography images. *Quantitative imaging in medicine and surgery* **2019**, *9*, 642.
- 79. Liu, N.; Fenster, A.; Tessier, D.; Gou, S.; Chong, J. Self-supervised learning enhanced ultrasound video thyroid nodule tracking. In Proceedings of the Medical Imaging 2023: Image Processing. SPIE, 2023, Vol. 12464, pp. 683–687.
- 80. Yadav, D.C.; Pal, S. Prediction of thyroid disease using decision tree ensemble method. *Human-Intelligent Systems Integration* **2020**, *2*, 89–95.
- 81. Zhao, R.N.; Zhang, B.; Yang, X.; Jiang, Y.X.; Lai, X.J.; Zhang, X.Y. Logistic regression analysis of contrast-enhanced ultrasound and conventional ultrasound characteristics of sub-centimeter thyroid nodules. *Ultrasound in medicine & biology* **2015**, *41*, 3102–3108.
- 82. Yazdani-Charati, J.; Akha, O.; Khosravi, F. Factors Affecting Thyroid Cancer in Patients with Thyroid Nodules Using Logistic Regression in Interval Censored Data. *International Journal of Cancer Management* **2018**, *11*.

83. Pavithra, R.; Parthiban, L. Optimal Deep Learning with Kernel Extreme Learning Machine Based Thyroid Disease Diagnosis and Classification Model. *Journal of Computational and Theoretical Nanoscience* **2021**, *18*, 639–649.
84. Rao, B.N.; Reddy, D.L.S.; Bhaskar, G. Thyroid Diagnosis Using Multilayer Perceptron. In Proceedings of the International Conference on E-Business and Telecommunications. Springer, 2019, pp. 452–459.
85. Hosseinzadeh, M.; Ahmed, O.H.; Ghafour, M.Y.; Safara, F.; Ali, S.; Vo, B.; Chiang, H.S.; et al. A multiple multilayer perceptron neural network with an adaptive learning algorithm for thyroid disease diagnosis in the internet of medical things. *The Journal of Supercomputing* **2020**, pp. 1–22.
86. Chandran, V.; Sumithra, M.; Karthick, A.; George, T.; Deivakani, M.; Elakkiya, B.; Subramaniam, U.; Manoharan, S. Diagnosis of Cervical Cancer based on Ensemble Deep Learning Network using Colposcopy Images. *BioMed Research International* **2021**, 2021.
87. Chen, D.; Hu, J.; Zhu, M.; Tang, N.; Yang, Y.; Feng, Y. Diagnosis of thyroid nodules for ultrasonographic characteristics indicative of malignancy using random forest. *BioData mining* **2020**, *13*, 1–21.
88. Himeur, Y.; Ghanem, K.; Alsaifi, A.; Bensaali, F.; Amira, A. Artificial intelligence based anomaly detection of energy consumption in buildings: A review, current trends and new perspectives. *Applied Energy* **2021**, *287*, 116601.
89. Mehta, P.; Bukov, M.; Wang, C.H.; Day, A.G.; Richardson, C.; Fisher, C.K.; Schwab, D.J. A high-bias, low-variance introduction to machine learning for physicists. *Physics reports* **2019**, *810*, 1–124.
90. Pan, Q.; Zhang, Y.; Zuo, M.; Xiang, L.; Chen, D. Improved ensemble classification method of thyroid disease based on random forest. In Proceedings of the 2016 8th International Conference on Information Technology in Medicine and Education (ITME). IEEE, 2016, pp. 567–571.
91. Chen, T.; Guestrin, C. Xgboost: A scalable tree boosting system. In Proceedings of the Proceedings of the 22nd ACM SIGKDD International Conference on Knowledge Discovery and Data Mining, 2016, pp. 785–794.
92. Guo, J.; Yang, L.; Bie, R.; Yu, J.; Gao, Y.; Shen, Y.; Kos, A. An XGBoost-based physical fitness evaluation model using advanced feature selection and Bayesian hyper-parameter optimization for wearable running monitoring. *Computer Networks* **2019**, *151*, 166–180.
93. Chen, Y.; Li, D.; Zhang, X.; Jin, J.; Shen, Y. Computer aided diagnosis of thyroid nodules based on the devised small-datasets multi-view ensemble learning. *Medical Image Analysis* **2020**, *67*, 101819.
94. Nobile, M.S.; Capitoli, G.; Sowirono, V.; Clerici, F.; Piga, I.; van Abeeelen, K.; Magni, F.; Pagni, F.; Galimberti, S.; Cazzaniga, P.; et al. Unsupervised neural networks as a support tool for pathology diagnosis in MALDI-MSI experiments: A case study on thyroid biopsies. *Expert Systems with Applications* **2023**, *215*, 119296.
95. Agrawal, U.; Soria, D.; Wagner, C.; Garibaldi, J.; Ellis, I.O.; Bartlett, J.M.; Cameron, D.; Rakha, E.A.; Green, A.R. Combining clustering and classification ensembles: A novel pipeline to identify breast cancer profiles. *Artificial intelligence in medicine* **2019**, *97*, 27–37.
96. Khan, A.R.; Khan, S.; Harouni, M.; Abbasi, R.; Iqbal, S.; Mehmmood, Z. Brain tumor segmentation using K-means clustering and deep learning with synthetic data augmentation for classification. *Microscopy Research and Technique* **2021**.
97. Yu, X.; Yu, G.; Wang, J. Clustering cancer gene expression data by projective clustering ensemble. *PloS one* **2017**, *12*, e0171429.
98. Chandel, K.; Kunwar, V.; Sabitha, A.S.; Bansal, A.; Choudhury, T. Analysing thyroid disease using density-based clustering technique. *International Journal of Business Intelligence and Data Mining* **2020**, *17*, 273–297.
99. Katikireddy Srinivas, D.K. Performa analysis of clustering of thyroid drug data using fuzzy and m-clust. *Journal of Critical Reviews* **2020**, *7*, 2128–2141.
100. Venkataramana, B.; Padmasree, L.; Rao, M.S.; Latha, D.; Ganesan, G. Comparative Study on performance of Fuzzy clustering algorithms on Liver and Thyroid Data. *Journal of Fuzzy Set Valued Analysis* **2018**, *2018*, 1–9.
101. Mahurkar, K.K.; Gaikwad, D. Normalization using Improvised K-Means applied in diagnosing thyroid disease with ANN. In Proceedings of the 2017 International Conference on Trends in Electronics and Informatics (ICETI). IEEE, 2017, pp. 579–583.
102. Yang, Y.; Song, Y.; Cao, B. An Information Entropy-based Method to Detect microRNA Regulatory Module. *IPSJ Transactions on Bioinformatics* **2019**, *12*, 1–8.

103. Kheddar, H.; Himeur, Y.; Awad, A.I. Deep transfer learning for intrusion detection in industrial control networks: A comprehensive review. *Journal of Network and Computer Applications* **2023**, *220*, 103760.
104. Canton, S.P.; Dadashzadeh, E.; Yip, L.; Forsythe, R.; Handzel, R. Automatic Detection of Thyroid and Adrenal Incidentallys Using Radiology Reports and Deep Learning. *Journal of Surgical Research* **2021**, *266*, 192–200.
105. Peng, S.; Liu, Y.; Lv, W.; Liu, L.; Zhou, Q.; Yang, H.; Ren, J.; Liu, G.; Wang, X.; Zhang, X.; et al. Deep learning-based artificial intelligence model to assist thyroid nodule diagnosis and management: a multicentre diagnostic study. *The Lancet Digital Health* **2021**, *3*, e250–e259.
106. Ferreira, M.F.; Camacho, R.; Teixeira, L.F. Autoencoders as weight initialization of deep classification networks applied to papillary thyroid carcinoma. In Proceedings of the 2018 IEEE International Conference on Bioinformatics and Biomedicine (BIBM). IEEE, 2018, pp. 629–632.
107. Teixeira, V.; Camacho, R.; Ferreira, P.G. Learning influential genes on cancer gene expression data with stacked denoising autoencoders. In Proceedings of the 2017 IEEE International Conference on Bioinformatics and Biomedicine (BIBM). IEEE, 2017, pp. 1201–1205.
108. Liu, T.; Guo, Q.; Lian, C.; Ren, X.; Liang, S.; Yu, J.; Niu, L.; Sun, W.; Shen, D. Automated detection and classification of thyroid nodules in ultrasound images using clinical-knowledge-guided convolutional neural networks. *Medical image analysis* **2019**, *58*, 101555.
109. Ha, E.J.; Baek, J.H.; Na, D.G. Deep convolutional neural network models for the diagnosis of thyroid cancer. *The Lancet Oncology* **2019**, *20*, e130.
110. Himeur, Y.; Al-Maadeed, S.; Kheddar, H.; Al-Maadeed, N.; Abualsaud, K.; Mohamed, A.; Khattab, T. Video surveillance using deep transfer learning and deep domain adaptation: Towards better generalization. *Engineering Applications of Artificial Intelligence* **2023**, *119*, 105698.
111. Li, X.; Zhang, S.; Zhang, Q.; Wei, X.; Pan, Y.; Zhao, J.; Xin, X.; Qin, C.; Wang, X.; Li, J.; et al. Diagnosis of thyroid cancer using deep convolutional neural network models applied to sonographic images: a retrospective, multicohort, diagnostic study. *The Lancet Oncology* **2019**, *20*, 193–201.
112. Xie, S.; Yu, J.; Liu, T.; Chang, Q.; Niu, L.; Sun, W. Thyroid Nodule Detection in Ultrasound Images with Convolutional Neural Networks. In Proceedings of the 2019 14th IEEE Conference on Industrial Electronics and Applications (ICIEA). IEEE, 2019, pp. 1442–1446.
113. Koh, J.; Lee, E.; Han, K.; Kim, E.K.; Son, E.J.; Sohn, Y.M.; Seo, M.; Kwon, M.r.; Yoon, J.H.; Lee, J.H.; et al. Diagnosis of thyroid nodules on ultrasonography by a deep convolutional neural network. *Scientific reports* **2020**, *10*, 1–9.
114. Liang, X.; Yu, J.; Liao, J.; Chen, Z. Convolutional Neural Network for Breast and Thyroid Nodules Diagnosis in Ultrasound Imaging. *BioMed Research International* **2020**, 2020.
115. Guan, Q.; Wang, Y.; Du, J.; Qin, Y.; Lu, H.; Xiang, J.; Wang, F. Deep learning based classification of ultrasound images for thyroid nodules: a large scale of pilot study. *Annals of Translational Medicine* **2019**, *7*.
116. Qiao, T.; Liu, S.; Cui, Z.; Yu, X.; Cai, H.; Zhang, H.; Sun, M.; Lv, Z.; Li, D. Deep learning for intelligent diagnosis in thyroid scintigraphy. *Journal of International Medical Research* **2021**, *49*, 0300060520982842.
117. ZHANG, Q.; HU, J.; ZHOU, S. The Detection of Hyperthyroidism by the Modified LeNet-5 Network. *Indian Journal of Pharmaceutical Sciences* **2020**, pp. 108–114.
118. Tekchandani, H.; Verma, S.; Londhe, N.D.; Jain, R.R.; Tiwari, A. Severity Assessment of Cervical Lymph Nodes using Modified VGG-Net, and Squeeze and Excitation Concept. In Proceedings of the 2021 IEEE 11th Annual Computing and Communication Workshop and Conference (CCWC). IEEE, 2021, pp. 0709–0714.
119. Chen, D.; Shi, C.; Wang, M.; Pan, Q. Thyroid Nodule Classification Using Hierarchical Recurrent Neural Network with Multiple Ultrasound Reports. In Proceedings of the International Conference on Neural Information Processing. Springer, 2017, pp. 765–773.
120. Yoo, T.K.; Choi, J.Y.; Kim, H.K. A generative adversarial network approach to predicting postoperative appearance after orbital decompression surgery for thyroid eye disease. *Computers in Biology and Medicine* **2020**, *118*, 103628.
121. Chandel, K.; Kunwar, V.; Sabitha, S.; Choudhury, T.; Mukherjee, S. A comparative study on thyroid disease detection using K-nearest neighbor and Naive Bayes classification techniques. *CSI transactions on ICT* **2016**, *4*, 313–319.
122. Ma, C.; Guan, J.; Zhao, W.; Wang, C. An efficient diagnosis system for Thyroid disease based on enhanced Kernelized Extreme Learning Machine Approach. In Proceedings of the International Conference on Cognitive Computing. Springer, 2018, pp. 86–101.

123. Xia, J.; Chen, H.; Li, Q.; Zhou, M.; Chen, L.; Cai, Z.; Fang, Y.; Zhou, H. Ultrasound-based differentiation of malignant and benign thyroid nodules: An extreme learning machine approach. *Computer methods and programs in biomedicine* **2017**, *147*, 37–49.
124. Dharmarajan, K.; Balasree, K.; Arunachalam, A.; Abirmai, K. Thyroid Disease Classification Using Decision Tree and SVM. *Executive editor* **2020**, *11*, 3234.
125. Yadav, D.C.; Pal, S. Decision tree ensemble techniques to predict thyroid disease. *Int. J. Recent Technol. Eng.* **2019**, *8*, 8242–8246.
126. Thomas, J.; Haertling, T. AIBx, artificial intelligence model to risk stratify thyroid nodules. *Thyroid* **2020**, *30*, 878–884.
127. Kezlarian, B.; Lin, O. Artificial Intelligence in Thyroid Fine Needle Aspiration Biopsies. *Acta Cytologica* **2020**, pp. 1–6.
128. Sanyal, P.; Mukherjee, T.; Barui, S.; Das, A.; Gangopadhyay, P. Artificial intelligence in cytopathology: a neural network to identify papillary carcinoma on thyroid fine-needle aspiration cytology smears. *Journal of pathology informatics* **2018**, *9*.
129. Yoon, J.; Lee, E.; Koo, J.S.; Yoon, J.H.; Nam, K.H.; Lee, J.; Jo, Y.S.; Moon, H.J.; Park, V.Y.; Kwak, J.Y. Artificial intelligence to predict the BRAFV600E mutation in patients with thyroid cancer. *PloS one* **2020**, *15*, e0242806.
130. Nguyen, D.T.; Kang, J.K.; Pham, T.D.; Batchuluun, G.; Park, K.R. Ultrasound image-based diagnosis of malignant thyroid nodule using artificial intelligence. *Sensors* **2020**, *20*, 1822.
131. Liu, T.; Xie, S.; Yu, J.; Niu, L.; Sun, W. Classification of thyroid nodules in ultrasound images using deep model based transfer learning and hybrid features. In Proceedings of the 2017 IEEE International Conference on Acoustics, Speech and Signal Processing (ICASSP). IEEE, 2017, pp. 919–923.
132. Abdolali, F.; Kapur, J.; Jaremko, J.L.; Noga, M.; Hareendranathan, A.R.; Punithakumar, K. Automated thyroid nodule detection from ultrasound imaging using deep convolutional neural networks. *Computers in Biology and Medicine* **2020**, *122*, 103871.
133. Li, X.; Wang, S.; Wei, X.; Zhu, J.; Yu, R.; Zhao, M.; Yu, M.; Liu, Z.; Liu, S. Fully convolutional networks for ultrasound image segmentation of thyroid nodules. In Proceedings of the 2018 IEEE 20th International Conference on High Performance Computing and Communications; IEEE 16th International Conference on Smart City; IEEE 4th International Conference on Data Science and Systems (HPCC/SmartCity/DSS). IEEE, 2018, pp. 886–890.
134. Kim, E.; Corte-Real, M.; Baloch, Z. A deep semantic mobile application for thyroid cytopathology. In Proceedings of the Medical Imaging 2016: PACS and Imaging Informatics: Next Generation and Innovations. International Society for Optics and Photonics, 2016, Vol. 9789, p. 97890A.
135. Ma, L.; Ma, C.; Liu, Y.; Wang, X. Thyroid diagnosis from SPECT images using convolutional neural network with optimization. *Computational intelligence and neuroscience* **2019**, *2019*.
136. Chai, Y.; Song, J.; Shear, M. Artificial Intelligence for thyroid nodule ultrasound image analysis. *Annals of Thyroid* **2020**, *5*.
137. Song, J.; Chai, Y.J.; Masuoka, H.; Park, S.W.; Kim, S.J.; Choi, J.Y.; Kong, H.J.; Lee, K.E.; Lee, J.; Kwak, N.; et al. Ultrasound image analysis using deep learning algorithm for the diagnosis of thyroid nodules. *Medicine* **2019**, *98*.
138. Barczyński, M.; Stopa-Barczyńska, M.; Wojtczak, B.; Czarniecka, A.; Konturek, A. Clinical validation of S-DetectTM mode in semi-automated ultrasound classification of thyroid lesions in surgical office. *Gland surgery* **2020**, *9*, S77.
139. Choi, Y.J.; Baek, J.H.; Park, H.S.; Shim, W.H.; Kim, T.Y.; Shong, Y.K.; Lee, J.H. A computer-aided diagnosis system using artificial intelligence for the diagnosis and characterization of thyroid nodules on ultrasound: initial clinical assessment. *Thyroid* **2017**, *27*, 546–552.
140. Fragogopoulos, C.; Pouliakis, A.; Meristoudis, C.; Mastorakis, E.; Margari, N.; Chroniaris, N.; Koufopoulos, N.; Delides, A.G.; Machairas, N.; Ntomi, V.; et al. Radial Basis Function Artificial Neural Network for the Investigation of Thyroid Cytological Lesions. *Journal of Thyroid Research* **2020**, *2020*.
141. Savala, R.; Dey, P.; Gupta, N. Artificial neural network model to distinguish follicular adenoma from follicular carcinoma on fine needle aspiration of thyroid. *Diagnostic cytopathology* **2018**, *46*, 244–249.
142. Li, L.R.; Du, B.; Liu, H.Q.; Chen, C. Artificial Intelligence for Personalized Medicine in Thyroid Cancer: Current Status and Future Perspectives. *Frontiers in Oncology* **2021**, *10*, 3360.
143. Zhao, Y.; Zhao, L.; Mao, T.; Zhong, L. Assessment of risk based on variant pathways and establishment of an artificial neural network model of thyroid cancer. *BMC medical genetics* **2019**, *20*, 1–10.

144. Wildman-Tobriner, B.; Buda, M.; Hoang, J.K.; Middleton, W.D.; Thayer, D.; Short, R.G.; Tessler, F.N.; Mazurowski, M.A. Using artificial intelligence to revise ACR TI-RADS risk stratification of thyroid nodules: diagnostic accuracy and utility. *Radiology* **2019**, *292*, 112–119.

145. Wang, L.; Yang, S.; Yang, S.; Zhao, C.; Tian, G.; Gao, Y.; Chen, Y.; Lu, Y. Automatic thyroid nodule recognition and diagnosis in ultrasound imaging with the YOLOv2 neural network. *World journal of surgical oncology* **2019**, *17*, 1–9.

146. Ozolek, J.A.; Tosun, A.B.; Wang, W.; Chen, C.; Kolouri, S.; Basu, S.; Huang, H.; Rohde, G.K. Accurate diagnosis of thyroid follicular lesions from nuclear morphology using supervised learning. *Medical image analysis* **2014**, *18*, 772–780.

147. Zhu, Y.; Sang, Q.; Jia, S.; Wang, Y.; Deyer, T. Deep neural networks could differentiate Bethesda class III versus class IV/V/VI. *Annals of translational medicine* **2019**, *7*.

148. Dolezal, J.M.; Trzcinska, A.; Liao, C.Y.; Kochanny, S.; Blair, E.; Agrawal, N.; Keutgen, X.M.; Angelos, P.; Cipriani, N.A.; Pearson, A.T. Deep learning prediction of BRAF-RAS gene expression signature identifies noninvasive follicular thyroid neoplasms with papillary-like nuclear features. *Modern Pathology* **2020**, pp. 1–13.

149. Daniels, K.; Gummadi, S.; Zhu, Z.; Wang, S.; Patel, J.; Swendseid, B.; Lyshchik, A.; Curry, J.; Cottrill, E.; Eisenbrey, J. Machine learning by ultrasonography for genetic risk stratification of thyroid nodules. *JAMA Otolaryngology—Head & Neck Surgery* **2020**, *146*, 36–41.

150. Tran, M.H.; Gomez, O.; Fei, B. A video transformer network for thyroid cancer detection on hyperspectral histologic images. In Proceedings of the Medical Imaging 2023: Digital and Computational Pathology. SPIE, 2023, Vol. 12471, pp. 32–41.

151. Gu, J.; Zhu, J.; Qiu, Q.; Wang, Y.; Bai, T.; Yin, Y. Prediction of immunohistochemistry of suspected thyroid nodules by use of machine learning-based radiomics. *American Journal of Roentgenology* **2019**, *213*, 1348–1357.

152. Colakoglu, B.; Alis, D.; Yergin, M. Diagnostic value of machine learning-based quantitative texture analysis in differentiating benign and malignant thyroid nodules. *Journal of oncology* **2019**, *2019*.

153. Park, V.Y.; Lee, E.; Lee, H.S.; Kim, H.J.; Yoon, J.; Son, J.; Song, K.; Moon, H.J.; Yoon, J.H.; Kim, G.R.; et al. Combining radiomics with ultrasound-based risk stratification systems for thyroid nodules: an approach for improving performance. *European Radiology* **2021**, *31*, 2405–2413.

154. Mughal, B.; Sharif, M.; Muhammad, N.; Saba, T. A novel classification scheme to decline the mortality rate among women due to breast tumor. *Microscopy research and technique* **2018**, *81*, 171–180.

155. Vaswani, A.; Shazeer, N.; Parmar, N.; Uszkoreit, J.; Jones, L.; Gomez, A.N.; Kaiser, Ł.; Polosukhin, I. Attention is all you need. *Advances in neural information processing systems* **2017**, *30*.

156. Lu, Y.; Yang, Y.; Chen, W. Application of deep learning in the prediction of benign and malignant thyroid nodules on ultrasound images. *IEEE Access* **2020**, *8*, 221468–221480.

157. Kwon, S.W.; Choi, I.J.; Kang, J.Y.; Jang, W.I.; Lee, G.H.; Lee, M.C. Ultrasonographic thyroid nodule classification using a deep convolutional neural network with surgical pathology. *Journal of digital imaging* **2020**, *33*, 1202–1208.

158. Chan, W.K.; Sun, J.H.; Liou, M.J.; Li, Y.R.; Chou, W.Y.; Liu, F.H.; Chen, S.T.; Peng, S.J. Using deep convolutional neural networks for enhanced ultrasonographic image diagnosis of differentiated thyroid cancer. *Biomedicines* **2021**, *9*, 1771.

159. Wang, X.; Agyekum, E.A.; Ren, Y.; Zhang, J.; Zhang, Q.; Sun, H.; Zhang, G.; Xu, F.; Bo, X.; Lv, W.; et al. A radiomic nomogram for the ultrasound-based evaluation of extrathyroidal extension in papillary thyroid carcinoma. *Frontiers in Oncology* **2021**, *11*, 625646.

160. Zhou, H.; Wang, K.; Tian, J. Online Transfer Learning for Differential Diagnosis of Benign and Malignant Thyroid Nodules with Ultrasound Images. *IEEE Transactions on Biomedical Engineering* **2020**.

161. Ma, J.; Wu, F.; Jiang, T.; Zhao, Q.; Kong, D. Ultrasound image-based thyroid nodule automatic segmentation using convolutional neural networks. *International journal of computer assisted radiology and surgery* **2017**, *12*, 1895–1910.

162. Chi, J.; Walia, E.; Babyn, P.; Wang, J.; Groot, G.; Eramian, M. Thyroid nodule classification in ultrasound images by fine-tuning deep convolutional neural network. *Journal of digital imaging* **2017**, *30*, 477–486.

163. Duc, N.T.; Lee, Y.M.; Park, J.H.; Lee, B. An ensemble deep learning for automatic prediction of papillary thyroid carcinoma using fine needle aspiration cytology. *Expert Systems with Applications* **2022**, *188*, 115927.

164. Ouyang, F.s.; Guo, B.l.; Ouyang, L.z.; Liu, Z.w.; Lin, S.j.; Meng, W.; Huang, X.y.; Chen, H.x.; Qiu-Gen, H.; Yang, S.m. Comparison between linear and nonlinear machine-learning algorithms for the classification of thyroid nodules. *European journal of radiology* **2019**, *113*, 251–257.

165. Zhao, C.K.; Ren, T.T.; Yin, Y.F.; Shi, H.; Wang, H.X.; Zhou, B.Y.; Wang, X.R.; Li, X.; Zhang, Y.F.; Liu, C.; et al. A comparative analysis of two machine learning-based diagnostic patterns with thyroid imaging reporting and data system for thyroid nodules: diagnostic performance and unnecessary biopsy rate. *Thyroid* **2021**, *31*, 470–481.

166. Vadhraj, V.V.; Simpkin, A.; O'Connell, J.; Singh Ospina, N.; Maraka, S.; O'Keeffe, D.T. Ultrasound image classification of thyroid nodules using machine learning techniques. *Medicina* **2021**, *57*, 527.

167. Gild, M.L.; Chan, M.; Gajera, J.; Lurie, B.; Gandomkar, Z.; Clifton-Bligh, R.J. Risk stratification of indeterminate thyroid nodules using ultrasound and machine learning algorithms. *Clinical Endocrinology* **2022**, *96*, 646–652.

168. Ma, J.; Wu, F.; Zhu, J.; Xu, D.; Kong, D. A pre-trained convolutional neural network based method for thyroid nodule diagnosis. *Ultrasonics* **2017**, *73*, 221–230.

169. Zhu, Y.; Fu, Z.; Fei, J. An image augmentation method using convolutional network for thyroid nodule classification by transfer learning. In Proceedings of the 2017 3rd IEEE international conference on computer and communications (ICCC). IEEE, 2017, pp. 1819–1823.

170. Gao, L.; Liu, R.; Jiang, Y.; Song, W.; Wang, Y.; Liu, J.; Wang, J.; Wu, D.; Li, S.; Hao, A.; et al. Computer-aided system for diagnosing thyroid nodules on ultrasound: A comparison with radiologist-based clinical assessments. *Head & neck* **2018**, *40*, 778–783.

171. Zuo, D.; Han, L.; Chen, K.; Li, C.; Hua, Z.; Lin, J. Extraction of calcification in ultrasonic images based on convolution neural network. *Sheng wu yi xue Gong Cheng xue za zhi= Journal of Biomedical Engineering= Shengwu Yixue Gongchengxue Zazhi* **2018**, *35*, 679–687.

172. Zhu, J.; Zhang, S.; Yu, R.; Liu, Z.; Gao, H.; Yue, B.; Liu, X.; Zheng, X.; Gao, M.; Wei, X. An efficient deep convolutional neural network model for visual localization and automatic diagnosis of thyroid nodules on ultrasound images. *Quantitative Imaging in Medicine and Surgery* **2021**, *11*, 1368.

173. Kim, Y.J.; Choi, Y.; Hur, S.J.; Park, K.S.; Kim, H.J.; Seo, M.; Lee, M.K.; Jung, S.L.; Jung, C.K. Deep convolutional neural network for classification of thyroid nodules on ultrasound: Comparison of the diagnostic performance with that of radiologists. *European Journal of Radiology* **2022**, *152*, 110335.

174. Lee, J.H.; Ha, E.J.; Kim, J.H. Application of deep learning to the diagnosis of cervical lymph node metastasis from thyroid cancer with CT. *European radiology* **2019**, *29*, 5452–5457.

175. Tsou, P.; Wu, C.J. Mapping driver mutations to histopathological subtypes in papillary thyroid carcinoma: applying a deep convolutional neural network. *Journal of clinical medicine* **2019**, *8*, 1675.

176. Kim, G.; Lee, E.; Kim, H.; Yoon, J.; Park, V.; Kwak, J. Convolutional neural network to stratify the malignancy risk of thyroid nodules: diagnostic performance compared with the American college of radiology thyroid imaging reporting and data system implemented by experienced radiologists. *American Journal of Neuroradiology* **2021**, *42*, 1513–1519.

177. Wu, G.G.; Lv, W.Z.; Yin, R.; Xu, J.W.; Yan, Y.J.; Chen, R.X.; Wang, J.Y.; Zhang, B.; Cui, X.W.; Dietrich, C.F. Deep learning based on ACR TI-RADS can improve the differential diagnosis of thyroid nodules. *Frontiers in Oncology* **2021**, *11*, 575166.

178. Jin, Z.; Zhu, Y.; Zhang, S.; Xie, F.; Zhang, M.; Zhang, Y.; Tian, X.; Zhang, J.; Luo, Y.; Cao, J. Ultrasound computer-aided diagnosis (CAD) based on the thyroid imaging reporting and data system (TI-RADS) to distinguish benign from malignant thyroid nodules and the diagnostic performance of radiologists with different diagnostic experience. *Medical Science Monitor: International Medical Journal of Experimental and Clinical Research* **2020**, *26*, e918452–1.

179. Park, V.Y.; Han, K.; Lee, E.; Kim, E.K.; Moon, H.J.; Yoon, J.H.; Kwak, J.Y. Association between radiomics signature and disease-free survival in conventional papillary thyroid carcinoma. *Scientific reports* **2019**, *9*, 4501.

180. Murphy, P.M. UCI repository of machine learning databases. <ftp://pub/machine-learning-databases.uci.edu> **1994**.

181. Kheddar, H. Transformers and large language models for efficient intrusion detection systems: A comprehensive survey. *arXiv preprint arXiv:2408.07583* **2024**.

182. Djeffal, N.; Kheddar, H.; Addou, D.; Mazari, A.C.; Himeur, Y. Automatic Speech Recognition with BERT and CTC Transformers: A Review. In Proceedings of the 2023 2nd International Conference on Electronics, Energy and Measurement (IC2EM). IEEE, 2023, Vol. 1, pp. 1–8.

183. Kheddar, H.; Hemis, M.; Himeur, Y. Automatic speech recognition using advanced deep learning approaches: A survey. *Information Fusion* **2024**, p. 102422.

184. Chi, J.; Li, Z.; Sun, Z.; Yu, X.; Wang, H. Hybrid transformer UNet for thyroid segmentation from ultrasound scans. *Computers in Biology and Medicine* **2023**, *153*, 106453.

185. Sharma, R.; Mahanti, G.K.; Panda, G.; Rath, A.; Dash, S.; Mallik, S.; Hu, R. A Framework for Detecting Thyroid Cancer from Ultrasound and Histopathological Images Using Deep Learning, Meta-Heuristics, and MCDM Algorithms. *Journal of Imaging* **2023**, *9*, 173.

186. Pathak, A.; Yu, Z.; Paredes, D.; Monsour, E.P.; Rocha, A.O.; Brito, J.P.; Ospina, N.S.; Wu, Y. Extracting Thyroid Nodules Characteristics from Ultrasound Reports Using Transformer-based Natural Language Processing Methods. *arXiv preprint arXiv:2304.00115* **2023**.

187. Bi, H.; Cai, C.; Sun, J.; Jiang, Y.; Lu, G.; Shu, H.; Ni, X. BPAT-UNet: Boundary preserving assembled transformer UNet for ultrasound thyroid nodule segmentation. *Computer Methods and Programs in Biomedicine* **2023**, *238*, 107614.

188. Chen, F.; Han, H.; Wan, P.; Liao, H.; Liu, C.; Zhang, D. Joint Segmentation and Differential Diagnosis of Thyroid Nodule in Contrast-Enhanced Ultrasound Images. *IEEE Transactions on Biomedical Engineering* **2023**.

189. Dov, D.; Assaad, S.; Si, S.; Wang, R.; Xu, H.; Kovalsky, S.Z.; Bell, J.; Range, D.E.; Cohen, J.; Henao, R.; et al. Affinitention nets: kernel perspective on attention architectures for set classification with applications to medical text and images. In Proceedings of the Proceedings of the Conference on Health, Inference, and Learning, 2021, pp. 14–24.

190. JERBI, F.; ABOUDI, N.; KHLIFA, N. Automatic classification of ultrasound thyroids images using vision transformers and generative adversarial networks. *Scientific African* **2023**, *20*, e01679.

191. Jiang, T.; Xing, W.; Yu, M.; Ta, D. A hybrid enhanced attention transformer network for medical ultrasound image segmentation. *Biomedical Signal Processing and Control* **2023**, *86*, 105329.

192. Li, G.; Chen, R.; Zhang, J.; Liu, K.; Geng, C.; Lyu, L. Fusing enhanced Transformer and large kernel CNN for malignant thyroid nodule segmentation. *Biomedical Signal Processing and Control* **2023**, *83*, 104636.

193. Liu, Q.; Ding, F.; Li, J.; Ji, S.; Liu, K.; Geng, C.; Lyu, L. DCA-Net: Dual-branch contextual-aware network for auxiliary localization and segmentation of parathyroid glands. *Biomedical Signal Processing and Control* **2023**, *84*, 104856.

194. Nam, J.; Choi, J.W.; Shin, Y.G.; Park, S. A BERT-Based Artificial Intelligence to Analyze Free-Text Clinical Notes for Binary Classification in Papillary Thyroid Carcinoma Recurrence. In Proceedings of the 2023 IEEE International Conference on Consumer Electronics (ICCE). IEEE, 2023, pp. 1–2.

195. Sun, J.; Wu, B.; Zhao, T.; Gao, L.; Xie, K.; Lin, T.; Sui, J.; Li, X.; Wu, X.; Ni, X. Classification for thyroid nodule using ViT with contrastive learning in ultrasound images. *Computers in Biology and Medicine* **2023**, *152*, 106444.

196. Tampu, I.E.; Eklund, A.; Johansson, K.; Gimm, O.; Haj-Hosseini, N. Diseased thyroid tissue classification in OCT images using deep learning: Towards surgical decision support. *Journal of Biophotonics* **2023**, *16*, e202200227.

197. Tao, Z.; Dang, H.; Shi, Y.; Wang, W.; Wang, X.; Ren, S. Local and context-attention adaptive LCA-Net for thyroid nodule segmentation in ultrasound images. *Sensors* **2022**, *22*, 5984.

198. Wang, Z.; Yu, L.; Ding, X.; Liao, X.; Wang, L. Shared-specific Feature Learning with Bottleneck Fusion Transformer for Multi-modal Whole Slide Image Analysis. *IEEE Transactions on Medical Imaging* **2023**.

199. Wang, Z.; Yu, L.; Ding, X.; Liao, X.; Wang, L. Lymph node metastasis prediction from whole slide images with transformer-guided multiinstance learning and knowledge transfer. *IEEE Transactions on Medical Imaging* **2022**, *41*, 2777–2787.

200. Xiao, N.; Li, Z.; Chen, S.; Zhao, L.; Yang, Y.; Xie, H.; Liu, Y.; Quan, Y.; Duan, J. Contrast-enhanced CT image synthesis of thyroid based on transformer and texture branching. In Proceedings of the 2022 5th International Conference on Artificial Intelligence and Big Data (ICAIBD). IEEE, 2022, pp. 94–100.

201. Yin, P.; Yu, B.; Jiang, C.; Chen, H. Pyramid Tokens-to-Token Vision Transformer for Thyroid Pathology Image Classification. In Proceedings of the 2022 Eleventh International Conference on Image Processing Theory, Tools and Applications (IPTA). IEEE, 2022, pp. 1–6.

202. Yu, B.; Yin, P.; Chen, H.; Wang, Y.; Zhao, Y.; Cong, X.; Dijkstra, J.; Cong, L. Pyramid multi-loss vision transformer for thyroid cancer classification using cytological smear. *Knowledge-Based Systems* **2023**, p. 110721.

203. Lee, D.T.; Vaid, A.; Menon, K.M.; Freeman, R.; Matteson, D.S.; Marin, M.P.; Nadkarni, G.N. Development of a privacy preserving large language model for automated data extraction from thyroid cancer pathology reports. *MedRxiv* **2023**, pp. 2023–11.

204. Raghunathan, R.; Jacobs, A.R.; Sant, V.R.; King, L.J.; Rothberger, G.; Prescott, J.; Allendorf, J.; Seib, C.D.; Patel, K.N.; Suh, I. Can large language models address unmet patient information needs and reduce provider burnout in the management of thyroid disease? *Surgery* **2025**, 177, 108859.

205. Wang, Z.; Zhang, Z.; Traverso, A.; Dekker, A.; Qian, L.; Sun, P. Assessing the role of GPT-4 in thyroid ultrasound diagnosis and treatment recommendations: enhancing interpretability with a chain of thought approach. *Quantitative Imaging in Medicine and Surgery* **2024**, 14, 1602.

206. Wu, S.H.; Tong, W.J.; Li, M.D.; Hu, H.T.; Lu, X.Z.; Huang, Z.R.; Lin, X.X.; Lu, R.F.; Lu, M.D.; Chen, L.D.; et al. Collaborative Enhancement of Consistency and Accuracy in US Diagnosis of Thyroid Nodules Using Large Language Models. *Radiology* **2024**, 310, e232255.

207. Shah, M.; Kuo, E.J.; Kuo, J.H.; Hsu, S.; McManus, C.; Liou, R.; Lee, J.A.; Sathe, T.S. EndoGPT: A Proof-of-concept Large Language Model Based Assistant for the Management of Thyroid Nodules. *medRxiv* **2024**, pp. 2024–05.

208. Yao, J.; Wang, Y.; Lei, Z.; Wang, K.; Li, X.; Zhou, J.; Hao, X.; Shen, J.; Wang, Z.; Ru, R.; et al. AI-Generated Content Enhanced Computer-Aided Diagnosis Model for Thyroid Nodules: A ChatGPT-Style Assistant. *arXiv preprint arXiv:2402.02401* **2024**.

209. Zhang, M.; Cheng, Q.; Wei, Z.; Xu, J.; Wu, S.; Xu, N.; Zhao, C.; Yu, L.; Feng, W. BertTCR: a Bert-based deep learning framework for predicting cancer-related immune status based on T cell receptor repertoire. *Briefings in Bioinformatics* **2024**, 25, bbae420.

210. Himeur, Y.; Varlamis, I.; Kheddar, H.; Amira, A.; Atalla, S.; Singh, Y.; Bensaali, F.; Mansoor, W. Federated Learning for Computer Vision. *arXiv preprint arXiv:2308.13558* **2023**.

211. Shah, A.A.; Malik, H.A.M.; Muhammad, A.; Alourani, A.; Butt, Z.A. Deep learning ensemble 2D CNN approach towards the detection of lung cancer. *Scientific Reports* **2023**, 13, 2987.

212. Salazar-Vega, J.; Ortiz-Prado, E.; Solis-Pazmino, P.; Gómez-Barreno, L.; Simbaña-Rivera, K.; Henriquez-Trujillo, A.R.; Brito, J.P.; Toulkeridis, T.; Coral-Almeida, M. Thyroid Cancer in Ecuador, a 16 years population-based analysis (2001–2016). *BMC cancer* **2019**, 19, 1–8.

213. Elmore, L.W.; Greer, S.F.; Daniels, E.C.; Saxe, C.C.; Melner, M.H.; Krawiec, G.M.; Cance, W.G.; Phelps, W.C. Blueprint for cancer research: Critical gaps and opportunities. *CA: A Cancer Journal for Clinicians* **2021**, 71, 107–139.

214. Park, S.H.; Choi, J.; Byeon, J.S. Key principles of clinical validation, device approval, and insurance coverage decisions of artificial intelligence. *Korean journal of radiology* **2021**, 22, 442.

215. Zhu, Y.C.; AlZoubi, A.; Jassim, S.; Jiang, Q.; Zhang, Y.; Wang, Y.B.; Ye, X.D.; Hongbo, D. A generic deep learning framework to classify thyroid and breast lesions in ultrasound images. *Ultrasonics* **2021**, 110, 106300.

216. Yao, J.; Lei, Z.; Yue, W.; Feng, B.; Li, W.; Ou, D.; Feng, N.; Lu, Y.; Xu, J.; Chen, W.; et al. DeepThyNet: A Multimodal Deep Learning Method for Predicting Cervical Lymph Node Metastasis in Papillary Thyroid Cancer. *Advanced Intelligent Systems* **2022**, 4, 2200100.

217. Sayed, A.N.; Himeur, Y.; Bensaali, F. From time-series to 2d images for building occupancy prediction using deep transfer learning. *Engineering Applications of Artificial Intelligence* **2023**, 119, 105786.

218. Wang, C.W.; Lin, K.Y.; Lin, Y.J.; Khalil, M.A.; Chu, K.L.; Chao, T.K. A soft label deep learning to assist breast cancer target therapy and thyroid cancer diagnosis. *Cancers* **2022**, 14, 5312.

219. Al-Qurayshi, Z.; Randolph, G.W.; Kandil, E. Cost-effectiveness of computed tomography nodal scan in patients with papillary thyroid carcinoma. *Oral oncology* **2021**, 118, 105326.

220. Dov, D.; Kovalsky, S.; Cohen, J.; Range, D.; Henao, R.; Carin, L. Thyroid cancer malignancy prediction from whole slide cytopathology images. *arXiv preprint arXiv:1904.00839* **2019**.

221. Halicek, M.; Shahedi, M.; Little, J.V.; Chen, A.Y.; Myers, L.L.; Sumer, B.D.; Fei, B. Head and neck cancer detection in digitized whole-slide histology using convolutional neural networks. *Scientific reports* **2019**, 9, 1–11.

222. Karsa, A.; Punwani, S.; Shmueli, K. An optimized and highly repeatable MRI acquisition and processing pipeline for quantitative susceptibility mapping in the head-and-neck region. *Magnetic Resonance in Medicine* **2020**, 84, 3206–3222.

223. Sardianos, C.; Varlamis, I.; Chronis, C.; Dimitrakopoulos, G.; Alsalemi, A.; Himeur, Y.; Bensaali, F.; Amira, A. The emergence of explainability of intelligent systems: Delivering explainable and personalized recommendations for energy efficiency. *International Journal of Intelligent Systems* **2021**, 36, 656–680.

224. Masuda, T.; Nakaura, T.; Funama, Y.; Sugino, K.; Sato, T.; Yoshiura, T.; Baba, Y.; Awai, K. Machine learning to identify lymph node metastasis from thyroid cancer in patients undergoing contrast-enhanced CT studies. *Radiography* **2021**, *27*, 920–926.

225. Lamy, J.B.; Sekar, B.D.; Guezennec, G.; Bouaud, J.; Séroussi, B. Intelligence artificielle explicable pour le cancer du sein: Une approche visuelle de raisonnement à partir de cas. In Proceedings of the EGC, 2020, pp. 457–466.

226. Poceviciute, M.; Eilertsen, G.; Lundström, C. Survey of XAI in Digital Pathology. *Artificial Intelligence and Machine Learning for Digital Pathology: State-of-the-Art and Future Challenges 2020*, *12090*, 56.

227. Sayed, A.N.; Bensaali, F.; Himeur, Y.; Houchati, M. Edge-Based Real-Time Occupancy Detection System through a Non-Intrusive Sensing System. *Energies* **2023**, *16*, 2388.

228. Alsalemi, A.; Himeur, Y.; Bensaali, F.; Amira, A. An innovative edge-based internet of energy solution for promoting energy saving in buildings. *Sustainable Cities and Society* **2022**, *78*, 103571.

229. Sayed, A.; Himeur, Y.; Alsalemi, A.; Bensaali, F.; Amira, A. Intelligent edge-based recommender system for internet of energy applications. *IEEE Systems Journal* **2021**, *16*, 5001–5010.

230. Sufian, A.; Ghosh, A.; Sadiq, A.S.; Smarandache, F. A survey on deep transfer learning to edge computing for mitigating the COVID-19 pandemic. *Journal of Systems Architecture* **2020**, *108*, 101830.

231. Rajan, J.P.; Rajan, S.E.; Martis, R.J.; Panigrahi, B.K. Fog computing employed computer aided cancer classification system using deep neural network in internet of things based healthcare system. *Journal of medical systems* **2020**, *44*, 1–10.

232. Kheddar, H.; Dawoud, D.W.; Awad, A.I.; Himeur, Y.; Khan, M.K. Reinforcement-Learning-Based Intrusion Detection in Communication Networks: A Review. *IEEE Communications Surveys & Tutorials* **2024**.

233. Balaprakash, P.; Egele, R.; Salim, M.; Wild, S.; Vishwanath, V.; Xia, F.; Brettin, T.; Stevens, R. Scalable reinforcement-learning-based neural architecture search for cancer deep learning research. In Proceedings of the Proceedings of the International Conference for High Performance Computing, Networking, Storage and Analysis, 2019, pp. 1–33.

234. Li, Z.; Xia, Y. Deep reinforcement learning for weakly-supervised lymph node segmentation in ct images. *IEEE Journal of Biomedical and Health Informatics* **2020**.

235. Kerdjidj, O.; Himeur, Y.; Sohail, S.S.; Amira, A.; Fadli, F.; Atalla, S.; Mansoor, W.; Copiaco, A.; Daradkeh, M.; Gawanmeh, A.; et al. Uncovering the Potential of Indoor Localization: Role of Deep and Transfer Learning **2023**.

236. Kheddar, H.; Himeur, Y.; Al-Maadeed, S.; Amira, A.; Bensaali, F. Deep transfer learning for automatic speech recognition: Towards better generalization. *Knowledge-Based Systems* **2023**, *277*, 110851.

237. Narayan, V.; Mall, P.K.; Alkhayyat, A.; Abhishek, K.; Kumar, S.; Pandey, P.; et al. Enhance-Net: An Approach to Boost the Performance of Deep Learning Model Based on Real-Time Medical Images. *Journal of Sensors* **2023**, *2023*.

238. Lee, H.; Chai, Y.J.; Joo, H.; Lee, K.; Hwang, J.Y.; Kim, S.M.; Kim, K.; Nam, I.C.; Choi, J.Y.; Yu, H.W.; et al. Federated learning for thyroid ultrasound image analysis to protect personal information: Validation study in a real health care environment. *JMIR medical informatics* **2021**, *9*, e25869.

239. Elharrouss, O.; Al-Maadeed, S.; Subramanian, N.; Ottakath, N.; AlMaadeed, N.; Himeur, Y. Panoptic segmentation: A review. *arXiv preprint arXiv:2111.10250* **2021**.

240. Yu, X.; Lou, B.; Zhang, D.; Winkel, D.; Arrahmane, N.; Diallo, M.; Meng, T.; von Busch, H.; Grimm, R.; Kiefer, B.; et al. Deep Attentive Panoptic Model for Prostate Cancer Detection Using Biparametric MRI Scans. In Proceedings of the International Conference on Medical Image Computing and Computer-Assisted Intervention. Springer, 2020, pp. 594–604.

241. Ivanova, D. Artificial Intelligence in Internet of Medical Imaging Things: The Power of Thyroid Cancer Detection. In Proceedings of the 2018 International Conference on Information Technologies (InfoTech). IEEE, 2018, pp. 1–4.

242. Borovska, P.; Ivanova, D.; Draganov, I. Internet of Medical Imaging Things and Analytics in Support of Precision Medicine for the Case Study of Thyroid Cancer Early Diagnostics. *Serdica Journal of Computing, Bulgarian Academy of Sciences, Institute of Mathematics and Informatics, accepted paper* **2018**.

243. Seifert, P.; Ullrich, S.L.; Kühnel, C.; Gühne, F.; Drescher, R.; Winkens, T.; Freesmeyer, M. Optimization of Thyroid Volume Determination by Stitched 3D-Ultrasound Data Sets in Patients with Structural Thyroid Disease. *Biomedicines* **2023**, *11*, 381.

244. Pakkasjärvi, N.; Luthra, T.; Anand, S. Artificial Intelligence in Surgical Learning. *Surgeries* **2023**, *4*, 86–97.

245. Bodenstedt, S.; Wagner, M.; Müller-Stich, B.P.; Weitz, J.; Speidel, S. Artificial intelligence-assisted surgery: potential and challenges. *Visceral Medicine* **2020**, *36*, 450–455.

246. Lee, D.; Yu, H.W.; Kwon, H.; Kong, H.J.; Lee, K.E.; Kim, H.C. Evaluation of Surgical Skills during Robotic Surgery by Deep Learning-Based Multiple Surgical Instrument Tracking in Training and Actual Operations. *Journal of clinical medicine* **2020**, *9*, 1964.

247. Himeur, Y.; Alsalemi, A.; Al-Kababji, A.; Bensaali, F.; Amira, A.; Sardianos, C.; Dimitrakopoulos, G.; Varlamis, I. A survey of recommender systems for energy efficiency in buildings: Principles, challenges and prospects. *Information Fusion* **2021**, *72*, 1–21.

248. Areeb, Q.M.; Nadeem, M.; Sohail, S.S.; Imam, R.; Doctor, F.; Himeur, Y.; Hussain, A.; Amira, A. Filter bubbles in recommender systems: Fact or fallacy—A systematic review. *Wiley Interdisciplinary Reviews: Data Mining and Knowledge Discovery* **2023**, p. e1512.

249. Varlamis, I.; Sardianos, C.; Chronis, C.; Dimitrakopoulos, G.; Himeur, Y.; Alsalemi, A.; Bensaali, F.; Amira, A. Smart fusion of sensor data and human feedback for personalized energy-saving recommendations. *Applied Energy* **2022**, *305*, 117775.

250. Atalla, S.; Daradkeh, M.; Gawanmeh, A.; Khalil, H.; Mansoor, W.; Miniaoui, S.; Himeur, Y. An Intelligent Recommendation System for Automating Academic Advising Based on Curriculum Analysis and Performance Modeling. *Mathematics* **2023**, *11*, 1098.

251. Habchi, Y.; Bouddou, R.; Aimer, A.F.; Beladgham, M. A New Cell Spreading Video Coding Based on Bandelet Transform and Lifting Scheme for Medical applications. *Przeglad Elektrotechniczny* **2023**, *99*.

252. Beladgham, M.; Habchi, Y.; Taleb-Ahmed, A.; et al. Medical video compression using bandelet based on lifting scheme and SPIHT coding: In search of high visual quality. *Informatics in Medicine Unlocked* **2019**, *17*, 100244.

253. Habchi, Y.; Aimer, A.F.; Baili, J.; Inc, M.; Menni, Y.; Lorenzini, G. Improving medical video coding using multi scale quincunx lattice: From low bitrate to high quality **2022**.

254. Habchi, Y.; Aimer, A.F.; Beladgham, M.; Bouddou, R. Ultra low bitrate retinal image compression using integer lifting scheme and subband encoder. *Indonesian Journal of Electrical Engineering and Computer Science (IJECS)* **2021**, *24*, 295–307.

255. Habchi, Y.; Beladgham, M.; Taleb-Ahmed, A. RGB Medical Video Compression Using Geometric Wavelet and SPIHT Coding. *International Journal of Electrical and Computer Engineering* **2016**, *6*, 1627–1636.

256. Boucherit, I.; Kheddar, H. Reinforced Residual Encoder–Decoder Network for Image Denoising via Deeper Encoding and Balanced Skip Connections. *Big Data and Cognitive Computing* **2025**, *9*, 82.

257. Gangwal, A.; Ansari, A.; Ahmad, I.; Azad, A.K.; Sulaiman, W.M.A.W. Current strategies to address data scarcity in artificial intelligence-based drug discovery: A comprehensive review. *Computers in Biology and Medicine* **2024**, *179*, 108734.

258. Kumar, T.; Brennan, R.; Mileo, A.; Bendechache, M. Image data augmentation approaches: A comprehensive survey and future directions. *IEEE Access* **2024**.

259. Huang, S.C.; Pareek, A.; Jensen, M.; Lungren, M.P.; Yeung, S.; Chaudhari, A.S. Self-supervised learning for medical image classification: a systematic review and implementation guidelines. *NPJ Digital Medicine* **2023**, *6*, 74.

260. Wolf, D.; Payer, T.; Lisson, C.S.; Lisson, C.G.; Beer, M.; Götz, M.; Ropinski, T. Self-supervised pre-training with contrastive and masked autoencoder methods for dealing with small datasets in deep learning for medical imaging. *Scientific Reports* **2023**, *13*, 20260.